Coordination Chemistry Reviews 253 (2009) 2193–2213

Contents lists available at ScienceDirect

Coordination Chemistry Reviews

journal homepage: www.elsevier.com/locate/ccr

Review

Supramolecular aggregates containing lipophilic Gd(III) complexes as contrast agents in MRI

Antonella Accardo[a], Diego Tesauro[a], Luigi Aloj[b], Carlo Pedone[a], Giancarlo Morelli[a,*]

[a] Department of Biological Sciences, CIRPeB University of Naples "Federico II", & IBB CNR, Via Mezzocannone 16, 80134 Naples, Italy
[b] Area Funzionale di Medicina Nucleare, Istituto Nazionale Tumori, Fondazione "G. Pascale", Via M. Semola, 80131 Naples, Italy

Contents

Abbreviations: AATZAC17, [6-bis(carboxymethyl)amino-4-carboxymethyl-6-heptadecyl-1,4-diazepan-1-yl]acetic acid; BME-DTTA, N^3,N^6-bis(2′-myristoyloxyethyl)-1,8-dioxo-triethylene-tetraamine-N,N,N′,N′-tetraacetic acid; BOPTA, 4-carboxy-5,8,11-tris(carboxymethyl)-1-phenyl-2-oxa-5,8,11-triazatridecan-13-oate; Chol, cholesterol; C_{18}DTPAGlu, α nonaoctanoyl, ε N,N-bis[2-[bis(carboxy-ethyl)amino]ethyl]-L-glutamyl lysine amide; $(C_{18})_2$DTPAGlu, α N,N-dioctadecylsuccinamyl, ε N,N-bis[2-[bis(carboxy-ethyl)amino]ethyl]-L-glutamyl lysine amide; DMPC, dimyristoylphosphatidylcholine; DMPG, dimyristoylphosphatidylglycerol; DO3A, 1,4,7,10-tetraazacyclododecane-1,4,7-triacetic acid; DOPC, 1,2-dioleoyl-sn-glycero-3-phosphocholine; DOPE-rhodamine, phosphatidylethanolamine lissamine rhodamine; DOTA, 1,4,7,10-tetraazacyclododecane-1,4,7,10-tetraacetic acid; DOTA-C10, 1,4,7,10-tetraaza-1-(1-carboxymethylundecane)-4,7,10-triacetic acid cyclododecane; DOTA-C12, 1,4,7,10-tetraaza-1-(1-carboxymethyltridecane)-4,7,10-triacetic acid cyclododecane; DOTA-C14, 1,4,7,10-tetraaza-1-(1-carboxymethylquintodecane)-4,7,10-triacetic acid cyclododecane; DOTA chol, DOTA-mono-(N-cholesteryloxy-3-carbonyl-1,2-diaminoethane)amide; DOTA·DSA, 2-{4,7-bis-carboxymethyl-10-[(N,N-distearylamidomethyl-N′-amidomethyl]-1,4,7,10 tetraazacyclododec-1-yl}acetic acid; DOTASAC12, 1,4,7,10-tetraazacyclododecane-1-(1′-carboxy-1′-dodecyl(methyl)amino-oxo-ethyl)-4,7,10-triacetic acid; DOTASAC18, 1,4,7,10-tetraazacyclododecane-1-(1′-carboxy-1′-octadecyl(methyl)amino-oxo-ethyl)-4,7,10-triacetic acid; DPPC, dipalmitoylphospatidylcholine; DPPG, dipalmitoylphosphatidylglycerol; DSPC, distearoylphosphatidylcholine; DSPE-PEG2000, 1,2-distearoyl-sn-glycero-3-phosphoethanolamine-N-[methoxy(polyethylene glycol)-2000]; DSPG, distearoylphosphatidylglycerol; DTPA, diethylenetriamine pentaacetic acid; DTPA-BC14, DTPA-bis-tetradecylamide; DTPA-BC16, DTPA-bis-hexadecylamide; DTPA-BC18, DTPA-bis-octadecylamide; DTPA-BMA, 1,7-bis[(N-methylcarbamoyl)methyl]-1,4,7-tris(carboxymethyl)-1,4,7-triazaheptane); DTPA-BPH, diethylenetriamine-N,N‴-di(acetyl-L-phenylalanine-hexadecylester)-N,N″,N‴-triacetic acid; DTPA-BPO, diethylenetriamine-N,N‴-di(acetyl-L-phenylalanineoc-tadecylester)-N,N″,N‴-triacetic acid; DTPA-BPT, diethylenetriamine-N,N‴-di(acetyl-L-phenylalaninete-tradecylester)-N,N″,N‴-triacetic acid; DTPA-BSA, DTPA-bis(oleylamide); DTPA-bis, (sterylamide); DTPAGlu, N,N-bis[2-[bis(carboxy-ethyl)amino]ethyl]-L-glutamic acid; DTPA-MC12, DTPA-monolaurylamide; DTPA-MC14, DTPA-monomyristylamide; DTPA-MC16, DTPA-mono-palmitylamide; DTPA-MC18, DTPA-monostearylamide; DTPA-PE, diethylenetriamine pentaacetic acid-phosphatidyl ethanolamine; DTPA-SA, diethylenetriaminepentaacetic acid-distearylamide; HDD-DO3A, 2-hydroxydodecyl-1,4,7-tris(carboxymethyl)-1,4,7,10-tetraazacyclododecane; EPTPA-C16, hydroxymethyl-hexadecanoyl ester)ethylene-propylenetriaminepentaacetic acid; HHD-DO3A, 2-hydroxyhexadecyl-1,4,7-tris(carboxymethyl)-1,4,7,10-tetraazacyclododecane; MPB-PE, 4-p-malimido phenyl butyryl] dioleoyl phosphatidylethanolamine; 1MP-DTTA, 1-[3′-(myristoyloxy)propyl]-diethylenetriamine-1,4,7,7-tetracetic acid; 4MP-DTTA, 4-[3′-(myristoyloxy)propyl]-diethylenetriamine-1,1,7,7-tetracetic acid; 4MPD-DTTA, 4-[3′-(myristoyloxy)propyl]-2,6-dioxodiethylenetriamine-1,1,7,7,-tetracetic acid; MRA, magnetic resonance angiography; MRI, magnetic resonance imaging; PCTA-[12], 12-dodecyloxy-3,6,9,15-tetraazabicyclo[9.3.1]pentadeca-1(15),11,13-triene-3,6,9-triacetic acid; PAA-b-PMA, poly(acrylic acid)-block-poly(methyl acrylate); PBFO, perfluorooctyl bromide; PEG-P(Asp), poly(ethylene glycol)-block-poly(aspartic acid); PLL-NGPE, poly(lysyl)glutaryl phosphatidyl ethanol-amine; PSI, polysuccinimide; TNFα, tumour necrosis factor-alpha; VEGF, vascular endothelial growth factor.

* Corresponding author. Tel.: +39 081 2536650; fax: +39 081 2536642.
E-mail address: gmorelli@unina.it (G. Morelli).

0010-8545/$ – see front matter
doi:10.1016/j.ccr.2009.01.015

ARTICLE INFO

Article history:
Received 8 October 2008
Accepted 18 January 2009
Available online 24 January 2009

Keywords:
Amphiphilic gadolinium complexes
MRI contrast agents
Micelles
Liposomes
Target-selective contrast agents

ABSTRACT

Magnetic resonance imaging (MRI) contrast agents based on paramagnetic gadolinium complexes are widely used in biomedical research and diagnosis. Their application is intended to improve efficacy of MRI providing physiological information along with the impressive anatomical detail already obtained by images without contrast. The classical gadolinium complexes currently used for MRI contrast enhancement are all low molecular weight compounds that rapidly equilibrate between the intra and extravascular spaces after intravenous administration. In order to obtain gadolinium-based agents with different pharmacokinetic properties, supramolecular aggregates such as micelles and liposomes have been recently proposed. Micelles and liposomes, obtained by the aggregation of lipophilic gadolinium complexes are here described, with the aim to correlate their structural and relaxometric properties. We report on the state of the art in the development of supramolecular aggregates obtained by self-assembly of lipophilic gadolinium complexes and aggregates in which lipophilic gadolinium complexes are assembled with surfactants. Moreover aggregates derivatized with bioactive molecules, such as peptides and antibodies, acting as target selective MRI contrast agents are described.

1. Introduction

Magnetic resonance imaging (MRI) is one of the most impressive non-invasive medical diagnostic imaging procedure currently in use. MRI is based on the same principles of nuclear magnetic resonance (NMR). It is based on the NMR signal generated by hydrogen nuclei present in water and its changes that are dependent on the chemical environment [1,2].

The use of a contrast agent (CA) in magnetic resonance imaging is aimed at improving diagnostic accuracy of these clinical studies by providing images that contain physiological information along with the exquisitely high anatomic detail commonly obtained in non-contrast-enhanced images [3,4]. Image contrast in MRI is related to the relaxation process of hydrogen nuclei of water molecules. It is governed by three parameters: proton density, longitudinal relaxation time T_1, and transverse relaxation time T_2. The variation in the proton density between tissues is small; therefore, most of the contrast measured in MRI images is based on the T_1 or T_2 relaxation times. Accordingly, pulse sequences are designed to obtain distribution maps that are representative of one of the two parameters and are commonly referred to as T_1- or T_2-weighted images. Contrast agents have been developed that can influence either of these relaxation rates in tissues and are commonly referred to as T_1-agents and the T_2-agents. The T_1-agents, commonly based on paramagnetic ions such as gadolinium(III) complexes, reduce the longitudinal relaxation time and increase the T_1 signal intensity giving a positive contrast [5]. Superparamagnetic compounds based on iron oxide (SPIO) are T_2-agents, they provide a negative contrast by decreasing T_2 signal intensity [6].

Relaxivity (r_1) describes the efficacy of the paramagnetic contrast agent, at 1 mM concentration, in changing the rate of water proton relaxation [7]. The relaxation is due to dipole–dipole interactions between the proton nuclear spins and the fluctuating local magnetic field that results from the paramagnetic metal center. The most common paramagnetic compounds are based on gadolinium complexes coordinated by chelating agents. The gadolinium atom has a high spin state due to seven unpaired electrons, moreover, the coordinating agents leave one or two free positions for water coordination in the nine-position coordination sphere of the gadolinium ion. Water molecules that are coordinated to the metal center give a direct contribution to relaxivity, while the bulk solvent molecules experience the paramagnetic effect when they diffuse around the metal center. These two interactions give the most important contributes to the observed relaxivity and are known as the inner-sphere relaxation rate and outer-sphere relaxation rate, respectively. In addition, water molecules may be retained in the periphery of the metal center by hydrogen bonds for a relatively long time without binding to the metal, this is known as the second-sphere relaxation effect [8–11]. The overall measured relaxivity (R_1^{obs}) is, thus, a result of different contributions as indicated by:

$$R_1^{obs} = R_{1p}^{IS} + R_{1p}^{OS} + R_1^{W} \quad (1)$$

where R_{1p}^{IS} and R_{1p}^{OS} are the inner-sphere and outer-sphere relaxation enhancement in the presence of the paramagnetic complex at 1 mM concentration, respectively, and R_1^{W} is the relaxation rate of the water solvent in the absence of the paramagnetic complex.

The four most important classical, clinically used, T_1-agents have a molecular weight around 600–700 Da and relaxivities between 4 and 5 $mM^{-1}\,s^{-1}$ at 20 MHz and 310 K (Fig. 1). They are based on chelating agents with a branched or cyclic structure such as diethylenetriaminepentaacetic acid (DTPA) or 1,4,7,10-tetraazacyclododecane-*N*,*N*,*N*,*N*-tetraacetic acid (DOTA), respectively. These CA are regarded as non-specific agents or extracellular fluid space (EFS) agents, they have very similar pharmacokinetic properties because they distribute in the extracellular fluid and are eliminated via glomerular filtration. They are particularly useful to delineate lesions in the brain as a result of disruption of the blood–brain barrier. Successively, two other derivatives of Gd-DTPA were introduced [12,13] (Fig. 2). These compounds feature increased lipophilicity due to the introduction of an aromatic substituent on the carbon backbone of the DTPA ligand. This modification significantly alters the pharmacokinetics and the biodistribution of these CA as compared to the parent compound, Gd-DTPA. These hepatobiliary agents have affinity towards human serum albumin and are specificially concentrated by hepatocytes. They are partially excreted through the biliary system and the kidneys. By comparing the structure of hepatic agents with that of EFS agents, the liver specificity can be ascribed to the pendent hydrophobic phenyl rings. These small molecular contrast agents have a major role in diagnostic imaging: they have promising targeting ability, diffusion and penetration and relaxivity that can be modified according to different physiological states. However, the relaxivity and the specificity of these agents are limited; hence, methods to increase their sensitivity and their targeting ability have to be employed. To cope with the surging demand for contrast agents in molecular imaging, tailor-made chelates are required to improve relaxivity through the modulation of the coordination environment around the Gd(III) center and, at the same time, to increase the specificity for the *in vivo* micro-environment and for selected tissues or cells [14]. For example, the effectiveness of Gd(III) complexes as CA may be significantly improved by using protein–chelate conjugates in which the metal complex is covalently attached to amino acid residues of the protein [15],

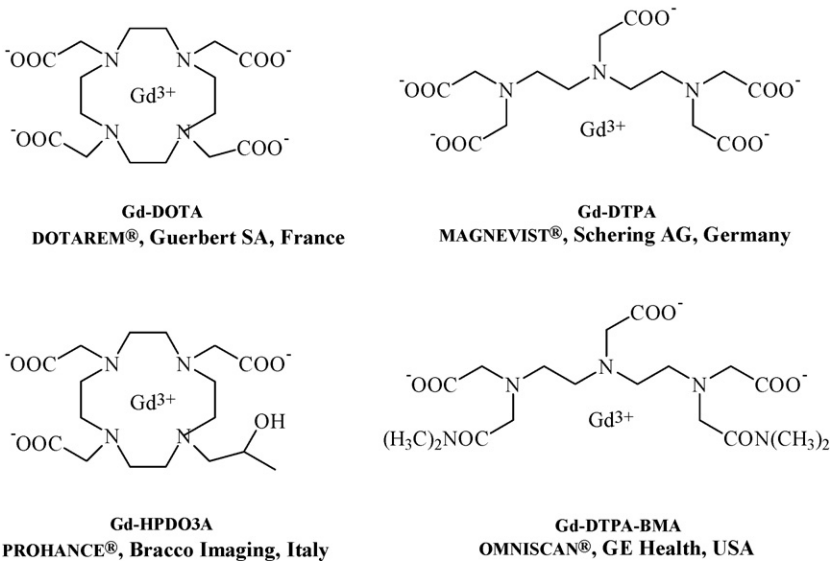

Fig. 1. Structures of the Gd(III)-based MRI contrast agents currently used in the clinical practice.

or by non-covalent binding of the complex to macromolecules [16]. This kind of approach allows one to couple the strong chelation of the metal ion with the slow molecular tumbling of macromolecules. According to the Solomon–Bloembergen–Morgan theory, an optimization of the water exchange rate, rotation and electronic paramagnetic relaxation, allows one to obtain a relaxivity of 100 $mM^{-1}\,s^{-1}$ for a complex with $q = 1$ at 20 MHz [11].

The research is now aimed in the development of new classes of contrast agents with improved properties such as smart contrast agents, target selective contrast agents and multimeric or macromolecular contrast agents [17,18]. "Smart or responsive contrast agents" are contrast agents in which a change in relaxivity is observed upon activation in the *in vivo* environment where they act [19]. They react to variables in their environment, such as temperature [20], pH [21–23], partial pressure of oxygen [24,25], metal ion concentration [26] or enzyme activity [27,28], giving a strong increase or decrease of the observed relaxivity. They are also used as tumour selective contrast agents for their responsive ability to tumour cell environment characterized by lower pH or by presence of different amounts of enzymes and proteins with respect to non-pathological environments. "Target selective contrast agents" are contrast agents in which the gadolinium complex is delivered in a selective way on cells or tissues of interest by bioactive molecules such as peptides and antibodies; in this approach the presence of specific receptors or membrane proteins overexpressed by cancer cells is the molecular target where the gadolinium complexes derivatized with peptides or antibodies are intended to accumulate [29,30].

In this review we will survey the MRI multimeric or macromolecular contrast agents in which a large number of gadolinium complexes are combined toghether and the total relaxivity results from the single contribution of each gadolinium ion [31,32].

We have devoted more attention to supramolecular aggregates, such as micelles and liposomes, attempting to suggest how to form aggregates with high relaxivity and stability. In particular in chapter four we will describe the three classes of non-specific contrast agents: (i) aggregates obtained directly by the self-assembly of amphiphilic chelating agents, (ii) mixed aggregates containing synthetic amphiphilic chelating agents and one or more commercial phospholipids, and (iii) self-assembling aggregates of polymeric amphiphiles that incorporate contrast agents. Finally in the fifth chapter we will evaluate target selective supramolecular aggregates, in which peptides or antibodies are present on the external surface of the aggregate for targeting molecules of biological interest expressed on the cell surface.

2. Multimeric or macromolecular contrast agents

The classical gadolinium complexes, currently available on the market, are all low molecular weight compounds that rapidly equilibrate between the intra and extravascular spaces after intravenous administration. In magnetic resonance angiography (MRA), intravascular contrast agents are utilized for applications such as

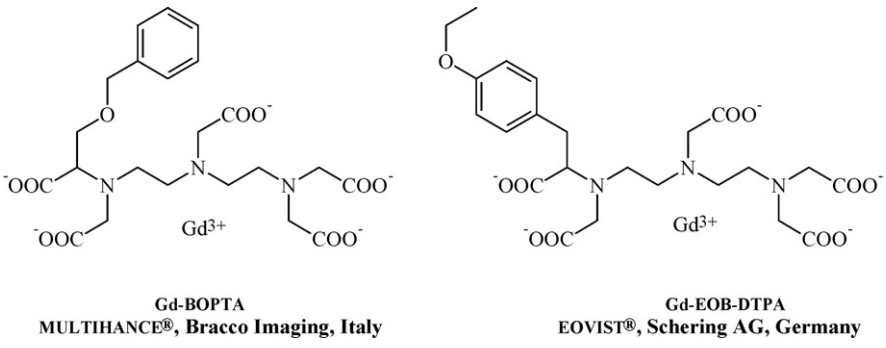

Fig. 2. Structures of two hepatobiliary agents which present pendent hydrophobic phenyl ring as aromatic substituent on the carbon backbone of the DTPA ligand.

coronary artery imaging [33,34] or for the assessment of other important features such as: relative blood volume of tissues, relative blood flow and endothelial permeability [35]. In fact, MRA is the technique in which blood vessels are imaged by magnetic resonance. Contrast-enhanced MRA provides a fast, reliable, non-invasive method for imaging large vascular structures, allowing one to evaluate pulmonary blood supply in patients with complex pulmonary stenosis and atresia, visualization and determination of the patency of coronary bypass grafts and renal artery stenosis, both in the native and in the transplanted kidney. In order to obtain a long residence time in blood of a gadolinium complex and increase the total relaxivity of the contrast agent, macromolecular and multimeric gadolinium complexes have been proposed so far.

A promising strategy is the insertion in the gadolinium complex, of a substituent capable of binding serum proteins. For example, the attachment of the protein-binding group diphenylcyclohexyl to a gadolinium(III) chelate via a phosphodiester linkage, like in the MS-325 contrast agent, results in reversible binding of MS-325 to human serum albumin in plasma (e.g. Angiomark®, Epix Medical or MP-2269, Mallinckrodt). The binding to human serum albumin reduces the extravasation of the contrast agent and also leads to a high increase in relaxivity [36]. Due to these properties, MS-325 provides strong, persistent enhancement of blood vessel images [37,38].

Other attempts to design blood pool contrast agents include synthesis of macromolecular gadolinium(III) chelates such as dendrimers [39], linear polymers [40], gadofullurenes [41], gadonanotubes [42], or large protein derivatives obtained by using the strong interaction present in the avidin–biotin complex [43], as schematized in Fig. 3. All of these are examples of contrast agents that remain confined to the blood vessel space because of their large molecular size. Moreover, the presence of a high number of gadolinium complexes for each molecule provides a great increase in relaxivity of the agent.

A similar approach is under investigation [44–46] with different dendrimeric compounds with varying sizes and properties. These macromolecules all contain gadolinium complexes on their perifery and are prepared employing relatively simple chemistry. The monodisperse character of dendrimers creates a unique opportunity to introduce dendritic MRI contrast agents into the clinic. For this approach as well the aim is to obtain high relaxivity and a prolonged vascular retention time given the large size of dendritic molecules (e.g. Gadomer®, Schering) [47].

Other polymers derivatized with stable gadolinium complexes have also been studied for their specific clinical applications and developed with the aim of obtaining molecules with extremely high relaxivity. For example the gadolinium-based polymers, gadolinium diethylenetriaminepentaacetic acid (DTPA)-co-1,6-diaminohexane (NC 22181) and Gd-DTPA-co-alpha, omega-diamino-polyethylene glycol(1450) (NC-66368), were formulated at a concentration of 80 mmol/L gadolinium and tested for use in lymphography in an animal model. Both compounds showed specific accumulation in the popliteal nodes of animal models after subcutaneous administration in the hind paw and were visualized using MRI [48].

Gadolinium-containing metallofullurenes, or gadofullurenes, have been proposed as a new generation of higher performance contrast agents for MRI [49–52]. The confinement of a Gd(III) ion within the fullerene cage prevents dissociation of the metal ion *in vivo*. Specifically, derivatized Gd@C60 nanoscale materials (1.0 nm diameter) offer new nanoscale paradigms for the design of high performance MRI contrast agent probes up to 20 times more effective than current clinical contrast agents [51]. In addition, *in vivo* biodistribution studies of the water-soluble Gd@C60 derivative have shown decreased uptake by the reticuloendothelial system (RES) and high-level clearance through the urinary system [52].

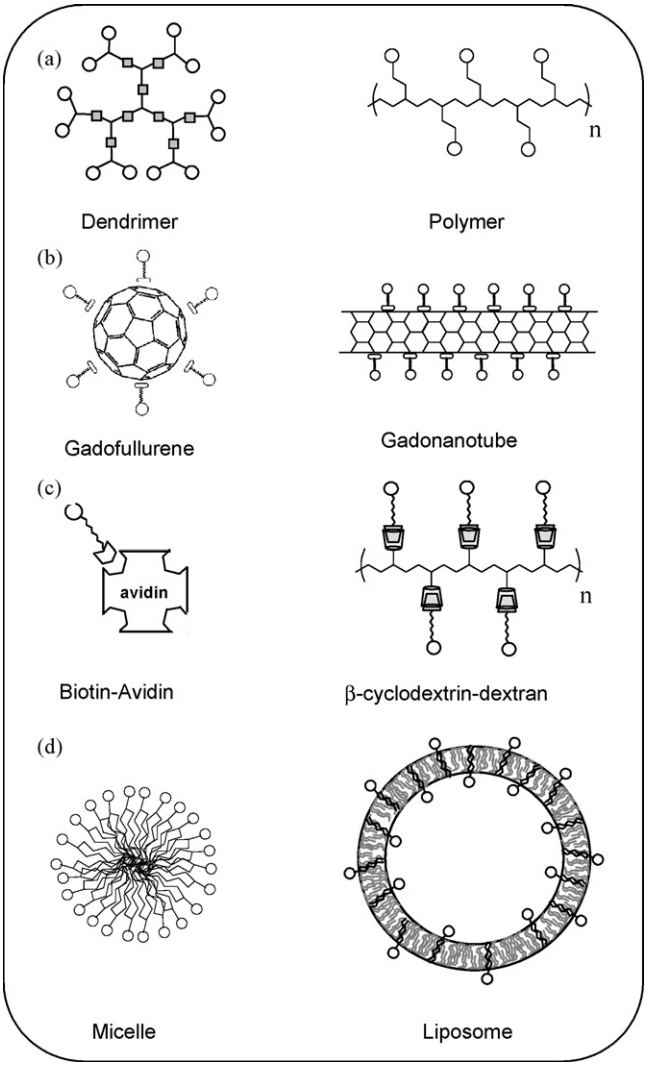

Fig. 3. Schematic representation of macromolecular adducts: (a) ramified or linear polymers; (b) carbon nanostructures (fullurenes and nanotubes) externally derivatized by stable gadolinium complexes; (c) macromolecular adducts obtained by non-covalent interactions between high molecular weight molecules such as protein or polymers and monomeric Gd(III) complexes; (d) supramolecular aggregates (micelles and liposomes) obtained by co-assembling of amphiphilic gadolinium complexes and one or more surfactants.

Another successful example of macromolecular systems is nanotubes. With their nanoscalar, superparamagnetic Gd(III) ion clusters (1×5 nm) confined within ultrashort (20–80 nm) single-walled carbon nanotube capsules, and their extremely high relaxivity, gadonanotubes are very effective T_1 agents. At 1.5 T, 37 °C, and pH 6.5, the r_1 relaxivity (ca. 180 $mM^{-1}\,s^{-1}$ per Gd(III) ion) of gadonanotubes is 40 times greater than any current gadolinium-based clinical agent [42]. Carbon nanotubes non-covalently functionalized by amphiphilic Gd chelates are powerful T_1 and T_2 MRI contrast agents [53]. The r_1 values are particularly high showing a strong dependence on the Gd complex concentration, particularly at low field. The proton relaxivities measured at 20 MHz with 0.1 and 0.05 mM GdL concentrations are 34.5 and 50.3 $mM^{-1}\,s^{-1}$, respectively.

A new approach has seen the use of macromolecular systems obtained by derivatizing the gadolinium complex with biotin. A biotinylated compound is associated to the protein avidin giving a macromolecular stable adduct containing four gadolinium complexes. This approach has been also used to develop target selective MRI contrast agents in which the supramolecular adduct is deliv-

ered on tumour cells endowed with avidin receptors [54]. Several systems based on the avidin–biotin recognition pathway have been recently considered as MRI probes. Bhujwalla and co-workers [55] have applied a two component Gd(III)-based avidin–biotin system for the visualization of HER-2 receptors in an experimental mouse model of breast carcinoma. Their approach consisted of targeting the extracellular domain of the receptors by means of a biotinylated antibody. After clearance of the unbound antibody, Gd(III)-labelled avidin is administered and binds to the biotinylated antibody with high affinity. The route based on the formation of non-covalent adducts may have several advantages, in particular those concerning accessibility and elimination pathways, compared to the use of macromolecular systems bearing covalent bound Gd(III) chelates. A similar non-covalent approach to prepare other macromolecular systems has been followed by using cyclodextrin and its organic ligands [56].

3. Micelles and liposomes

Micelles and liposomes are supramolecular aggregates (Fig. 4) obtained by spontaneous assembling in aqueous solution of amphiphilic molecules consisting of a hydrophobic and a hydrophilic moiety. The major forces that direct the self-assembly of amphiphilic molecules into well-defined structures in water derive from the hydrophobic associative interactions of the tails and the repulsive interactions between the hydrophilic head-groups [57]. There is a wide variability in both the hydrophobic and hydrophilic moieties of amphiphilic molecules. The hydrophobic part can vary in length and can consist of multiple chains, creating different ratios between the size of the hydrophobic and hydrophilic parts. Moreover, the size and charge of the polar head-group can vary, dividing these molecules into ionic (anionic or cationic) or non-ionic amphiphiles. Ninham and co-workers developed an empirical model based on a surfactant parameter (P) to predict aggregate type in solution based on the steric relationship of head-group and side arm size [58]. The surfactant parameter, $P = v/al$ depends from head-group surface area, the volume and length of the side chains (a, v and l respectively). A value $0.5 < P < 1$ predicts vesicles and $P < 0.5$ predicts micelle formation. To favour vesicular aggregation the head-group surface area (a parameter) should be decreased or the volume of the hydrophobic moiety (v parameter) should be increased. These characteristics and other parameters such as pH, ionic strength, temperature and concentration, determine the geometry of the aggregate that is formed in aqueous solution and whether a micelle-like structure (spherical, cylindrical, or ellipsoidal micelles) or a bilayer-like structure (open bilayers, vesicles, or liposomes) will be formed.

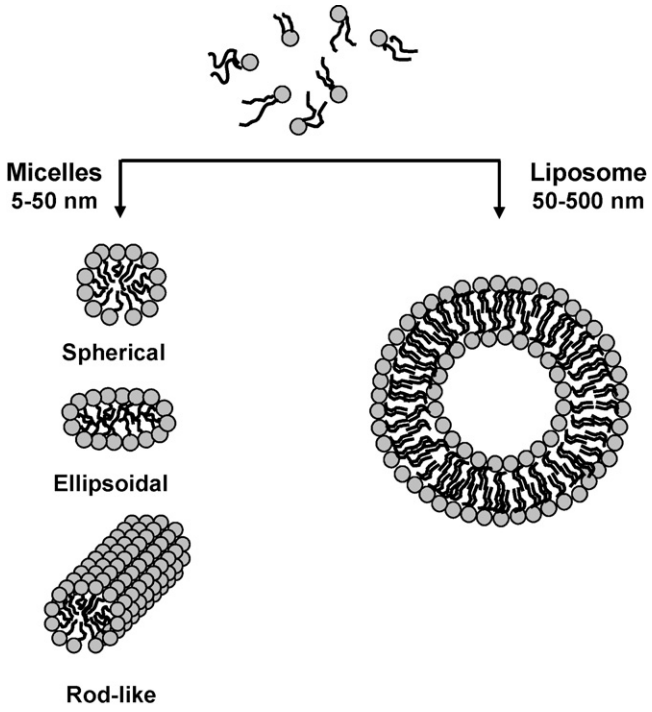

Fig. 4. Schematic representation of supramolecular aggregates (micelles and liposomes) obtained by assembling in aqueous solution amphiphilic molecules consisting of a hydrophobic and a hydrophilic moiety. More common size and shape of these aggregates are also reported.

In more detail, micellar aggregates are characterized by their unique core–shell architecture, where in an aqueous environment the hydrophobic fragment of the amphiphilic molecules is segregated from the aqueous exterior to form the inner core, and the hydrophilic part forms the corona or the outer shell. The formation of micelles is driven by the decrese of of free energy in the system because of the removal of hydrophobic fragment from the aqueous environment and the re-estabilishing of hydrogen bond network in water. Additional energy gain results from formation of Van der Waals bonds between hydrophobic moieties in the core of the formed micelles [59,60]. Micelles size normally varies between 5 and 50–100 nm and fills the gap between such drug carriers as individual macromolecules (antibodies, albumin, find a dextran) with the size below 5 nm and nanoparticulates (liposomes, microcapsules) with the size ca. 50 nm and up. Important characteristics of micelles are the concentration where they are formed, i.e., the critical micellar concentration (cmc), kinetic features such as the micellar lifetime, and their aggregation number. Cmc is the first identifiable physical change in solution-containing surfactants, as their concentration is increased, and represents the concentration of a monomeric amphiphile at which micelles appear. Optimal cmc value should be in a micromolar or low millimolar region.

On the other hand, liposomes are self-enclosed artificial phospholipid vesicles that vary in size from 50 to 1000 nm. They can be formed by one (unilamellar) or more concentric lipid bilayers (multilamellar) with an aqueous phase inside and between the lipid bilayers [61]. Unilamellar vesicles (UVs) can be divided according to their size in small (SUV, diameter of 50–150 nm) and large (LUV, diameter 150–800 nm) liposomes. The length of the hydrophobic moieties and the presence of unsaturated bonds in the phospholipid chains are two of the most important parameters that influence water permeability (P_w) of liposome membrane. The water permeability of liposomes decreases with increasing length of the phospholipid alkyl chain. In addition the presence of one or more unsaturations in the hydrocarbon chain reduces the tightness of the bilayer assembly, thus facilitating the water flux across the bilayer. Stabilization of the lipid bilayer is often aided by the addition of cholesterol that also influences P_w [62].

3.1. Paramagnetic aggregates as T_1-agents

Micelles and liposomes have recently drawn much attention owing to their structural properties can be easily controlled thus allowing favourable pharmacological characteristics. The biodistribution of micelles and liposomes is highly dependent on their physicochemical properties such as size, surface charge or membrane composition [63–66]. In the pursuit of different *in vivo* delivery purposes, one can easily change the size, charge and surface properties of these carriers simply by adding new ingredients to the mixture of amphiphilic substances used in their preparation and/or by changing the preparation methods. However, conventional micelles and liposomes are to a large extent taken-up by the RES. These properties make supramolecular aggregates excellent candidates as possible carriers of Gd(III)-chelates to enhance

the contrast efficacy and to change the pharmacokinetic properties of MRI contrast agents, and in the 1980s the first studies on the use of liposomes as carriers of MRI contrast agents appeared in the literature [67–69]. There have been two main approaches at the development of liposomal contrast agents: in the first one, contrast agents are entrapped within the internal aqueous space of liposomes [67]; in the second approach, lipophilic contrast agents are incorporated in the lipid bilayer of the liposome [68,69]. Classical gadolinium complexes such as Gd-DTPA, Gd-DTPA-BMA and Gd-HPDO3A have been loaded within the internal aqueous space of lipid vesicles: the main target for such supramolecular aggregates is the liver, given the avid accumulation of these aggregates by Kupffer cells, and the relatively slow clearance of the gadolinium complexes once internalized [70]. While studying blood concentrations of these aggregates to evaluate the possibility of using these liposomes for MRA application, it was observed that the enhancement of relaxivity is limited as it is approximately two to five times lower compared to the same concentrations of free gadolinium complexes in solution. The relaxivity of the entrapped paramagnetic species appears to be lowered because of the limited exchange of bulk water with the contrast agents [67,71] under these conditions. This slow exchange is caused by the low permeability of the liposomal membrane to water [72]. Thus the second approach, where a hydrophilic chelating agent is covalently linked to a hydrophobic chain, may be more effective. In this scheme, the lipid part of the molecule is anchored in the liposome bilayer while the more hydrophilic gadolinium complex is localized on the liposome surface [73,74]. Several chelating probes of this type have been developed for liposome membrane incorporation studies: DTPA-PE [75], DTPA-SA [76], amphiphilic acylated paramagnetic complexes of Mn and Gd [70]. This approach results in an improved ionic relaxivity of the metal compared to the approach of encapsulating the paramagnetic molecules in the aqueous interior liposomial space, and compared with low molecular weight complexes [77]. All the above reported macromolecular contrast agents have been also derivatized by using reporter molecules in order to have target selctive contrast agents and some of them have shown interesting properties for their high relaxivity, biodistribution profile and target selectivity.

3.2. Relaxivity of supramolecular contrast agents

The NMRD profile of supramolecular contrast agents shows a typical peak at higher frequencies, in agreement with the increase in the rotational correlation times as compared with low molecular weight Gd(III) chelates. This means that, at clinically relevant field strengths, these contrast agents have the highest gadolinium relaxivity. Furthermore, the amount of Gd(III) complexes per particle is high (varying from 50 atoms for small micelles to several hundred or thousand of atoms for liposomes). This enhances the total relaxivity per contrast agent particle enormously. As for classical gadolinium complexes, the most important parameters for understanding the relaxivity of supramolecular contrast agents are the rotational correlation time τ_R, the coordination number, q, the exchange rate τ_M and the electronic relaxation time T_{iE}.

The rotational correlation time τ_R is strictly related to the size and to the rigidity of the investigated system. A lengthened rotational correlation time τ_R can be achieved by incorporating the Gd(III)-complex into the liposomal membrane: this structural organization reduces the molecular tumbling of the contrast agent thus increasing τ_R. For the analysis of the longitudinal ^{17}O and ^{1}H relaxation rates of the aggregates, the Solomon–Bloembergen–Morgan model, modified according to the Lipari–Szabo approach should be used [78,79]. According to the Lipari–Szabo approach, the modulation of the interaction that causes relaxation is the result of two statistically independent motions: a rapid local motion of the Gd(III) complex, with a local rotational correlation time τ_l, and a slower global motion of the entire micellar aggregate, with a global rotational correlation time τ_g. The degree of spatial restriction of the local motion with regard to the global rotation is given by an additional model-free parameter, S^2. For a totally free internal motion $S^2 = 0$, while for a local motion that is exclusively correlated to the global motion $S^2 = 1$. Both the global and the local rotational correlation times are influenced by the length and by the hydrophobicity of the side chain in the amphiphilic gadolinium complex.

The coordination number, q, and the exchange rate, $\tau_{M,}$ determine the amount of water molecules that can effectively coordinate the Gd(III) ion and thereby increase the relaxation rate T_{1M}. In micellar structures the gadolinium complexes are entirely exposed on the external surface of the aggregate, while in liposomes gadolinium complexes are distributed between the inner and the outer compartment of the liposomes. The number of paramagnetic complex molecules embedded in the inner and outer layers of the liposomes could be different, and two different contributions arising respectively from the complexes in the inner and in the outer layers have to be considered. If the water exchange rate through the membrane is very slow, the main relaxation effect is expected to be due to the complex in the outer layer [51,67]. On the contrary, if this water exchange is extremely fast, complexes in the inner and in the outer layer will both contribute to the observed paramagnetic relaxation rate. The water exchange rate through the membrane is highly dependent on the permeability [72]. The more permeable the membrane, the better is the water flux across the bilayer and the higher the relaxivity [67]. Furthermore, the exchange with external bulk water can be improved by using smaller liposomes. The reduction in relaxivity with the use of large liposomes might be attributed to the reduced surface area-to-volume ratio and the presence of multilamellar bilayers, which slow down the water exchange between interior and exterior of the liposome [67,71]. This implies that in terms of relaxation properties, an optimal formulation would be liposomes of small size with a permeable bilayer. Unfortunately, permeable liposomes usually are less stable in serum than liposomes with more rigid bilayer.

4. Supramolecular aggregates containing lipophilic Gd(III) complexes as MRI contrast agents

Contrast agents based on supramolecular aggregates reported in literature can be divided into at least three categories: in the first one, aggregates are obtained directly by the self-assembly of an amphiphilic chelating agent; in the second one, aggregates are obtained by mixing a synthetic amphiphilic chelating agent with one or more commercial phospholipids; in the third example, the formulations based on the self-assembly of polymeric amphiphiles functionalized with the contrast agent.

4.1. Self-assembling aggregates of amphiphilic Gd(III) complexes

Amphiphilic gadolinium complexes are represented by a chelating agent covalently bound to a hydrophobic moiety such as a long alkyl chain or an organic molecule that promotes the aggregation process in a water-based solution. The chelating agent should complex the gadolinium ion with high stability. Generally, the kind of aggregate obtained by self-assembly of amphiphilic gadolinium complexes are micelles. In micelles, the Gd(III) complexes are exposed to the hydrophilic exterior space; therefore, there is easy access of the bulk water to the paramagnetic center.

Most of the amphiphilic Gd(III) complexes are composed of a gadolinium complex covalently bound to one or more alkylic chains. The structural properties of the hydrophobic chain such as its length

and its nature can influence the stability, the size and the aggregation number of monomers in the micelle. Moreover, the relaxivity behaviour of micelles can dramatically change as a function of the hydrophobic moiety.

Several studies were carried out on amphiphilic chelating agents in order to determine the most accurate mathematical approach to study the rotational dynamics of the aggregates, and to justify the relaxivity values. Between 1999 and 2002, Merbach and co-workers described the synthesis and relaxometric characterization of five potential Gd(III)-based MRI contrast agents which are capable of micellar self-organization. They mainly differ in the length of their side chain, varying between 10 and 18 carbon atoms. Three of them, **1**–**3**, $[Gd(DOTAC10)(H_2O)]^-$, $[Gd(DOTAC12)(H_2O)]^-$ and $[Gd(DOTAC14)(H_2O)]^-$ are DOTA-like chelates bearing a simple alkyl chain with 10, 12 and 14 carbon atoms. The other two, **4**–**5**, $[Gd(DOTASAC12)(H_2O)]$ and $[Gd(DOTASAC18)(H_2O)]$ have a DOTA chelating unit and a monoamide-dodecyl or a monoamide-octadecyl carbon side chain, respectively [80,81]. As stated above, for the analysis of the longitudinal ^{17}O and ^1H relaxation rates of the aggregates, the authors used the Solomon–Bloembergen–Morgan model, modified according to the Lipari–Szabo approach. The relaxivity values of the five micellar systems are reported in Table 1. It is interesting to underline that the relaxivity increases with increasing chain length within the series, with the exception of $[Gd(DOTASAC18)(H_2O)]^-$. This effect can be explained by the different rotational motions (global and local) and by the model-free parameter S^2 of the five systems. As expected, the global rotational correlation time, τ_g, increases with increasing length of the side chain (τ_g = 1600, 2220, 2810 ps, for $[Gd(DOTAC12)(H_2O)]^-$, $[Gd(DOTAC14)(H_2O)]^-$, $[Gd(DOTASAC18)(H_2O)]^-$, respectively). On the other hand, the local motions, that are also influenced by length and the hydrophobicity of the side chain, do not follow the expected behaviour: in fact in $[Gd(DOTASAC18)(H_2O)]^-$ micelles the additional amide function, prevents strong hydrophobic interactions between the long chains and reduces its internal flexibility (short τ_1 value and low S^2).

The relaxivity value of the supramolecular aggregate is influenced not only by their hydrophobic moiety, but also by the chelating agent on the head-group. For example, the relaxivity value strongly increases from 18.0 to 29.2 $mM^{-1}\,s^{-1}$, simple by replacing the DOTA with the PCTA chelating agent [82], notwithstanding the two monomers Gd-PCTA-[C12] and DOTASAC12 (indicated in Table 1 as **6** and **5**, respectively) have the same hydrophobic chain, the same coordination geometry on the gadolinium ion and aggregation properties (micelles with a similar critical micellar concentration in the 1.5–3.4 × 10^{-4} M range).

Clearly the micellization of amphiphilic gadolinium complexes gives rise to a system with slower molecular tumbling respect to the monomeric complex, but the resulting relaxivity appears still lower than the expected values as internal motions are faster than the overall tumbling of the micellar system. Merbach and co-workers demonstrated in 2003 that interactions between nearby paramagnetic centers in micellar systems increase the transverse electronic relaxation of the electronic spin of Gd(III) and, therefore, reduce the attainable water proton relaxivity [83]. This drawback can be removed by diluting the Gd(III) ions with diamagnetic Y(III) ions in order to increase the distance between the neighbouring Gd(III) ions. This theory was also recently confirmed by Aime et al. for micellar aggregates obtained by self-assembling of the Gd-AATZAC17 amphiphilic gadolinium complex **7**. They studied how the relaxivity value of micellar aggregates of Gd-AATZAC17 (30.0 $mM^{-1}\,s^{-1}$) changes when 98% of the Gd(III) complexes on the external surface of the micelles is replaced by the corresponding Y(III) complexes. The result observed was an enhancement in relaxivity of around 40% over the entire frequency range (41.4 $mM^{-1}\,s^{-1}$) [84].

Very recently, Geraldes et al. reported an "*in vitro*" characterization and "*in vivo*" animal imaging studies on self-assembling micelles of Gd-EPTPA-C16 monomer **8**. The *in vivo* results were compared with the commercially available low molecular mass Magnevist® [85]. The synthesis and the relaxometric characterization of the supramolecular system were previously reported from the authors [86]. The critical micellar concentration (3 × 10^{-4} M) of the amphiphilic $[(Gd\text{-}EPTPA\text{-}C16)(H_2O)]^{2-}$ chelate was determined by variable-concentration proton relaxivity measurements. The rotational dynamics of the micelles, analyzed by using the Lipari–Szabo approach, suggests that micelles formed in aqueous solution show considerable flexibility, with a local rotational correlation time of τ_1 = 330 ps and a global rotational correlation time τ_g = 2100 ps. These values are in good agreement with the results above described for **1**–**5** compounds. The *in vivo* evaluation of the micellar $[Gd(EPTPA\text{-}C16)(H_2O)]^{2-}$ compound in Wistar rats shows a persistent hepatic positive-contrast effect in T_1-weighted images, which is qualitatively similar to that of the clinically established Gd(III)-based hepatobiliary agents, Gd-EOB-DTPA [87] and Gd-BOPTA [88]. The possibility of using this type of micellar compound for imaging disease depends on the degree of stability of the imaging agent in the body relative to its critical micellar concentration. The amphiphilic gadolinium complexes above described have only one hydrophobic chain. Critical micellar concentration of mono-tailed surfactants is usually in the range of 0.1–0.01 mM. Upon dilution in the blood following injection, these aggregates may not be sufficiently stable and disassemble immediately following administration. Hence, there is a need to find a new class of surfactant molecules able to form more stable micelles with lower critical micellar concentration values. One of the possible candidates for this role, can be represented by aggregates obtained by self-assembling of monomers with two or more alkyl chains.

Recently, Paduano et al. reported supramolecular aggregates, constituted basically by the DTPAGlu moiety bound to a hydrophobic double-tail (18 carbon atoms), **9**. The amphiphilic molecule behaves as an anionic surfactant, and is capable of forming aggregates of different sizes and shapes (rodlike micelles, threadlike micelles, and vesicles) in aqueous solution by varying the method of preparation and the environmental conditions such as pH and ionic strength. A micelle-to-vesicle transition was observed by decreasing the pH value from 7.4 to 3.0; and/or by increasing the ionic strength. Relaxivity values of Gd-$(C18)_2$DTPAGlu aggregates at pH 7.4 in the presence and absence of NaCl at physiological ionic strength were 21.5 and 24.0 $mM^{-1}\,s^{-1}$, respectively [89,90]. An alternative approach to prepare physiologically stable aggregates include the use of Gd-labelled polymerized liposomes, prepared by using a polymerizable amphiphilic Gd–diethylenetriaminepenta acetic acid (Gd–DTPA) derivative [91]. Liposomes were prepared from amphiphilic molecules all containing a diacetylene triple bond in the fatty acyl chains. Then, to increase their stability, the triple bond-containing lipids were irradiated by UV light to induce chain–chain polymerization. These systems showed an improved physical stability, originated from the increased membrane rigidity and were able to avoid, to some extent, uptake by RES.

In the literature there are few examples of supramolecular aggregates obtained also by starting from amphiphilc gadolinium complexes in which the hydrophobic moiety is not represented by an alkyl chain, but from an organic molecule such as cholesterol. In 2003 Lattuada et al. reported the synthesis of Gd-DTPA·Chol **10**. The relaxivity value in water (27.2 $mM^{-1}\,s^{-1}$), extremely high compared to the relaxivity of the Gd-DTPA (3.7 $mM^{-1}\,s^{-1}$), is an indirect evidence of a micellar self-organization of the Gd-DTPA·Chol [92]. In 2006 Jorgensen et al. synthesized and studied the relaxivity behaviour of another cholesterol-based gadolinium lipid Gd-DOTA·Chol **11**, in which the chelating agent is represented by the DOTA. This molecule was designed to be easily embed-

Table 1
Relaxivity values, r_1, at 20 MHz and 25 °C, of self-assembling aggregates obtained by amphiphilic Gd(III) complexes.

Prinicipal investigator and reference	Compound name	#	Schematic representation of amphiphilic gadolinium complexes	r_1 ($mM^{-1}\ s^{-1}$)
A.E. Merbach [80,81]	Gd-DOTAC10	**1**	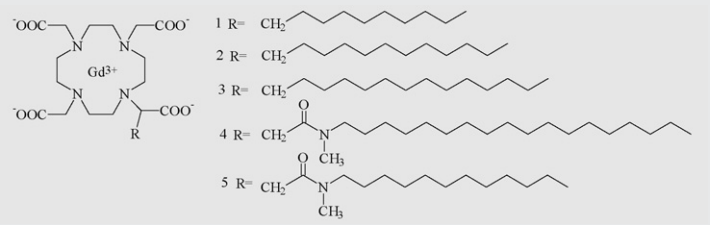	9.3
	Gd-DOTAC12	**2**		17.2
	Gd-DOTAC14	**3**		21.5
	Gd-DOTASAC18	**4**		20.7
	Gd-DOTASAC12	**5**		18.0
C. Glogard [82]	Gd-PCTA-[12]	**6**	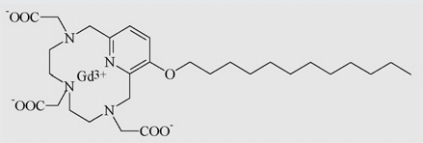	29.2
S. Aime [84]	Gd-AAZTAC17	**7**	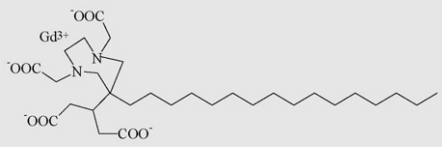	30.0
E. Tóth [85,86]	Gd-EPTPA-C16	**8**	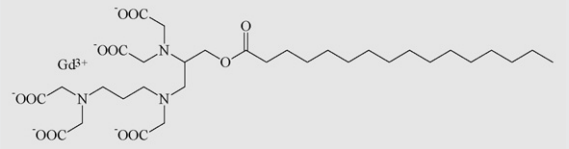	22.6
L. Paduano [89]	Gd-$(C18)_2$DTPAGlu	**9**	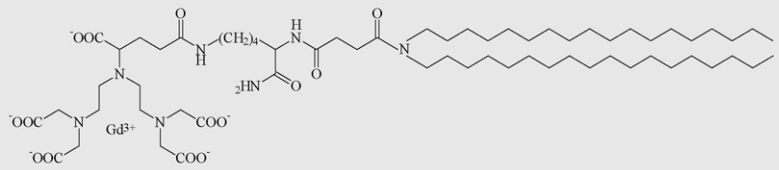	21.5
L. Lattuada [92]	Gd-DTPA·Chol	**10**	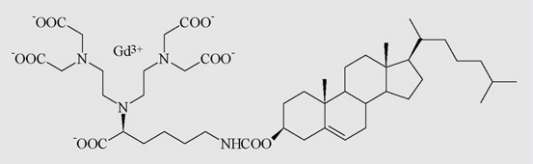	27.2
A.D. Jorgensen [93]	Gd-DOTA·Chol	**11**	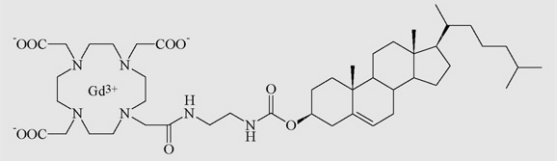	4.42[a]

[a] Compound **11** maintains a monomeric form, and its relaxivity value is lower than those presented by compounds that assemble into aggregates, as expected.

ded into the membrane of standard cationic liposomes in order to develop a liposome cell labelling system, which would be amenable to labelling a variety of cells, and could serve other purposes such as delivery of plasmid DNA or other nucleic acid derived therapeutics. The relaxivity of Gd-DOTA·Chol (4.42 $mM^{-1}\ s^{-1}$) is in the same order of values of the clinically used Dotarem (5.25 $mM^{-1}\ s^{-1}$), thus indicating the Gd-DOTA·Chol is unable to self-aggregate [93]. The uncapability of Gd-DOTA·Chol, with respect to Gd-DTPA·Chol, to self-aggregate can be ascribed to the lack of anionic charges on the complex that reduces the amphiphylic character of the molecule.

4.2. Mixed aggregates of amphiphilic Gd(III) complexes

Another class of supramolecular aggregates containing gadolinium complexes could be obtained by the co-assembling of amphiphilic gadolinium molecules with one or more commercial surfactants such as phospholipids, non-ionic surfactants or

cholesterol. Classical phospholipids can be divided in saturated (DPPC, DSPC, DSPE) and unsaturated (DOPC, POPC) molecules. The most common components of phospholipids are phosphatidyl choline (PC), phosphatidyl glycerol (PG) and phosphatidyl ethanolamine (PE). Generally, the presence of phospholipids within the supramolecular aggregate favours the formation of bilayer structures such as vesicles or liposomes. One of the first examples of supramolecular aggregates obtained by amphiphilic gadolinium complexes mixed to phospholipids was reported in 1992 from Elgavish et al. They synthesized several amphiphilic gadolinium monomers (1MP-DTTA; 4MP-DTTA; 4MPD-DTTA; BME-DTTA) and studied the *in vitro* relaxometric behaviour and the *in vivo* properties of mixed liposomes as potential contrast agents for MRI of myocardial under-perfusion [77,94–96]. Gd-BME-DTTA gadolinium complex, **12**, was obtained by conjugating the DTTA chelating moiety to two long fatty myristoyl chains. Because of its limited solubility in water, Gd-BME-DTTA complex was incorporated into egg lecithin liposomes. The median lethal dose (LD_{50}) of liposomal Gd-BME-DTTA formulation in mice was of 0.56 ± 0.05 mmol/kg and no deleterious effects on heart rate, blood pressure, left ventricular force and AV conductance in ferret hearts *in vivo* at the magnetic resonance imaging effective dose of 0.05 mmol/kg body weight were detected. In MRI images, a ^1H signal intensity enhancement was observed in the following organs in decreasing order of the effect: heart ≈ spleen > kidney > liver. This enhancement remained stable for over 3 h in all organs. Moreover, the incorporation of Gd-BME-DTTA in liposomes produced an increase of the *in vitro* relaxivity of the contrast agent up to 27.0 mM^{-1} s^{-1}. In anyway, the relaxivity of a liposomal Gd-BME-DTTA sample, stored at 4 °C, remained stable for over 4 months of observation, but a significant decrease in relaxivity (8.2 mM^{-1} s^{-1} after 40 days) was observed in a sample stored at room temperature. The observed time-dependent reduction in relaxivity can be possibly attributed to the dissociation of Gd-BME-DTTA from the phospholipid bilayer. Thus, liposome stability and relaxivity properties of the aggregate over the time are strongly related to the incorporation degree of amphiphilic gadolinium complex in the liposome membrane.

At this purpose, recently Gløgård et al. investigated the effect on the relaxivity of several parameters including the incorporation degree of the Gd(III) amphiphilic chelates on the membrane packing. They studied mixed liposomes formulated by using several phospholipid molecules (DMPC, DPPC, DSPC, DMPG, DPPG, DSPG) in which two amphiphilic Gd(III)-DO3A derivatives previously synthesized were alternatively introduced [97]. Gd-HDD-DO3A **13** and Gd-HHD-DO3A **14** (see Table 2) were synthesized by functionalizing DO3A chelating agent with hydroxydodecyl and hydroxyhexadecyl moieties, respectively. In the different formulations, the amount of cholesterol and the type of Gd(III)-chelate, were varied between 0–40 and 1–10% mol/mol, respectively. The incorporation efficacy seems to be directly correlated to the lipophilic moiety of the chelates. In fact, Gd-HHD-DO3A, with the highest partition (*P*) coefficient between 1-octanol and water, was completely incorporated whereas an incorporation efficacy between 12 and 23% was observed for the less lipophilic Gd-HDD-DO3A. Moreover, larger liposomes showed only a minor positive effect on the incorporation efficacy, while the cholesterol content has no effect on the Gd-chelate loading [98]. In disagree with the expected results, the relaxivity value decreased with the increase of incorporation degree of Gd(III) complex. An explanation of this result could be the negative influence of the Gd(III)-chelate on the membrane packing in the sense of creating disorder. A likely impact of this is an increase in the lateral surface motion on the liposome surface, leading to a shortening of τ_R for the Gd(III)-chelates and thereby a decrease in the relaxivity. The same authors also reported on the influence of the cholesterol content on the structure and relaxivity of aggregates obtained by Gd-HHD-DO3A molecules [99].

The incorporation degree of amphiphilic gadolinium complexes in liposomes represents only one of the numerous parameters that can play an important role in the relaxivity behaviour of liposomes. Strictly related to the incorporation degree is the mobility degree of the amphiphilic gadolinium complex, which depends from the length and from the location of the alkylic chains on the Gd(III) complex. In this contest, Binnemans et al. between 2003 and 2006 reported the synthesis of three different sets of amphiphilic derivatives of DTPA with alkyl chains of different length. The gadolinium(III) complexes of these ligands were incorporated into mixed aggregates of DPPC phospholipid and Tween 80 to obtain supramolecular structures. In the first set, the amphiphilic gadolinium complexes are represented by DTPA-bisamide derivatives with alkyl chains containing 14, 16 and 18 carbon atoms (Gd-DTPA-BC14, Gd-DTPA-BC16 and Gd-DTPA-BC18, see Table 2, compounds **15**–**17**) [100]. In the second set, the DTPA-bisamide derivatives were replaced by the DTPA-monoamide ones (Gd-DTPA-MC12, Gd-DTPA-MC14, Gd-DTPA-MC16 and Gd-DTPA-MC18, compounds **18**–**21**) [101]. Finally, in the last set the DTPA-bisamide derivatives were modified by introducing aromatic side chain groups (DTPA-BPT; DTPA-BPH and DTPA-BPO, **22**–**24**) [102]. By comparing the τ_M and τ_R values of the three sets of aggregates resulted that the relaxivity values of mixed aggregates incorporating monoamide complexes are higher than aggregates incorporating bisamide compounds of the same chain length. Both τ_M and τ_R values of Gd-DTPA-MCn monoamide supramolecular aggregates are smaller than those of Gd-DTPA-BCn and Gd-DTPA-BPX. Indeed it is well known that Gd-DTPA derivatives with amide groups are characterized by a decreased exchange rate of the coordinated water molecule and that τ_M is related to the number of amide functions and their substituents [103]. On the other hand the τ_R values decrease as a consequence of a more efficient immobilization of the paramagnetic part of the bisamide derivatives caused by the incorporation of both hydrophobic chains into the micellar or liposomial membrane. These smaller τ_R values are not followed by a decrease but by an increase in relaxivity because of the smaller τ_M values. The immobilization of bisamide derivatives at eighteen carbon atoms (Gd-DTPA-BC18 and Gd-DTPA-BPO) inside the supramolecular structure is less effective, probably because the aliphatic chains of the complex are longer than the alkyl chains of DPPC, in which it is inserted, resulting in a relatively high local mobility. The corresponding paramagnetic aggregates at 14 carbon atoms DTPA-BPT showed the highest relaxivity, most likely because the optimal length match between the hydrophobic chains of the DPPC and the amphiphilic gadolinium complex allowed very efficient packing of the paramagnetic complex into the aggregate. Mixed micelles incorporating Gd-DTPA-MC12 amphiphilic monomer show a relaxivity value (5.0 mM^{-1} s^{-1}) more similar to its parent compound Gd-DTPA than the supramolecular aggregtes. It can be explained by comparing the τ_R values obtained for the complex Gd-DTPA-MC12 (0.105 ns) in the micellar solution with respect to those of the other complexes of the series (0.91–1.12 ns). This result indicates that this complex is either very loosely incorporated inside the micellar membrane or not incorporated at all. It seems that the aliphatic chain of this complex is too short and the hydrophobic character of the complex too low to allow efficient incorporation into the micellar structures. Finally, the same authors studied a new compound (compound **25**, Table 2), Gd-DTPA-BC18Aunsat, containing C=C double bond in the two lipophilic chains [104]. The presence of the unsatured bond, as reported above, increases the flexibility inside the membrane layers and the water permeability, thus increasing relaxivity.

The other parameters influencing the relaxivity are represented by the membrane composition of aggregates, such as the saturation level of membrane, the transition phase temperature of phospho-

Table 2
Relaxivity values, r_1, at 20 MHz and 37–39 °C, of liposomal aggregates obtained by amphiphilic Gd(III) complexes.

Prinicipal investigator and reference	Compound name	#	Schematic representation of amphiphilic gadolinium complexes	r_1 ($mM^{-1}\ s^{-1}$)
G.A. Elgavish [77]	Gd-BME-DTTA	**12**	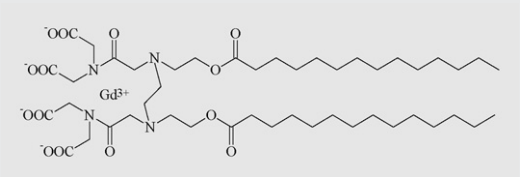	27.0[a]
C. Gløgård [97]	Gd-HDD-DO3A	**13**	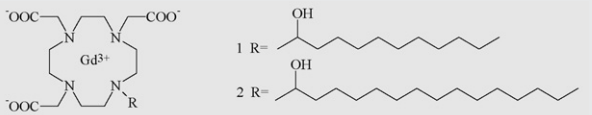	4.6[b]
	Gd-HHD-DO3A	**14**		9.2[b]
R.N. Muller [100]	Gd-DTPA-BC14	**15**	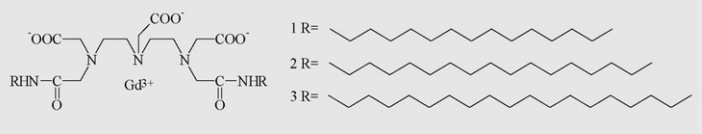	13.3
	Gd-DTPA-BC16	**16**		13.3
	Gd-DTPA-BC18	**17**		8.7
R.N. Muller [101]	Gd-DTPA-MC12	**18**	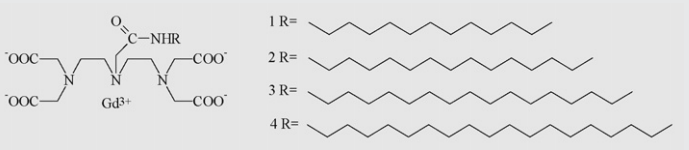	5.0
	Gd-DTPA-MC14	**19**		15.2
	Gd-DTPA-MC16	**20**		16.6
	Gd-DTPA-MC18	**21**		16.6
T.N. Parac-Vogt [102]	Gd-DTPA-BPT	**22**	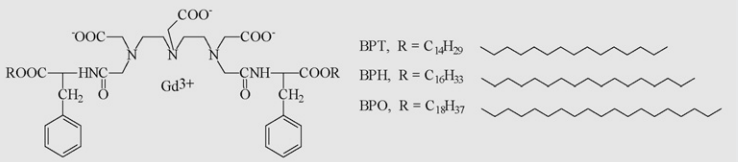	11.4
	Gd-DTPA-BPH	**23**		9.7
	Gd-DTPA-BPO	**24**		7.3
R.N. Muller [104]	Gd-DTPA-BC18Aunsat	**25**	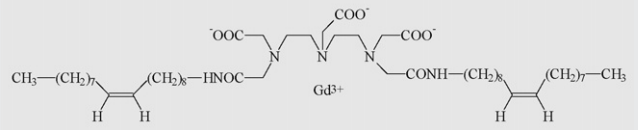	17.8
H. Tournier [108,109]		**26**		18.0
		27	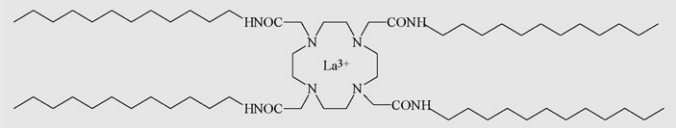	–

A.D. Miller [114]	**28**	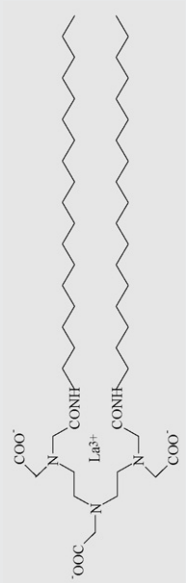	23.0
Gd-DOTA-DSA	**29**	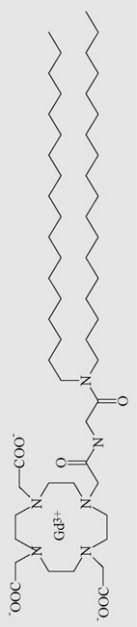	4.10[b]

[a] Value measured at 25 °C.
[b] The relaxivity values are given for compound in monomeric state: concentration below their cmc.

lipid and the cholesterol content. As above reported, gadolinium complexes incorporated in liposome bilayer can distribute them on both sides of the phospholipidic membrane and the two contributions arising respectively from the complexes in the inner and in the outer layers have to be considered. The two contributions depend from liposome membrane permeability which is strictly related to the bilayer composition (saturated or unsaturated phospholipids). Saturated phospholipids present a lower membrane permeability with respect to the liposome obtained by unsaturated phospholipids [72,105]. The reason for such a behaviour is due to the different packing of the hydrophobic chains in the bilayer. The presence of an unsaturation in the hydrocarbon chain reduces the tightness of the bilayer assembly, thus facilitating the water flux across the bilayer and improving the relaxivity. When the liposome membrane permeability is high, the water exchange will be extremely fast and both the complex in the inner and in the outer layer will contribute to the observed paramagnetic relaxation rate [106]. On the contrary, if the membrane permeability is low, water exchange rate through the membrane is very slow and the main relaxation effect will be due to the complex in the outer layer. This means that the relaxivity of unsaturated lipids will be higher compared to those obtained by saturated lipids, because of the higher accessibility of the water. This theory was very recently confirmed by Muller et al. The authors compared the relaxometric behaviour of two unilamellar liposomes (DPPC/compound **15** in Table 2 = 10/1), incorporating Gd(III) amphiphilic complexes either in their external and internal layers or only at the external one. Mixed liposomes with the Gd(III) complexes located only in the external part were successfully obtained by transmetallation of La(III) by Gd(III) ions of DPPC/La-DTPA-BC14 liposomes. The relaxivity of these liposomes (16.98 mM^{-1} s^{-1}) is increased as compared to that of the liposomes containing the complex in both sides of the membrane (9.86 mM^{-1} s^{-1}), thus indicating the complex located in the internal layer contributes less to the global relaxivity [107]. The water permeability (P_w) of liposomes can be also strongly influenced by the incorporation of amphiphilic gadolinium complexes in the lipid bilayer, as reported by Aime et al. Two liposome formulations (DPPC/DSPE-PEG2000 and POPC/Chol/DSPE-PEG2000) were selected in order to compare the variation of the P_w factor between the saturated and unsaturated liposomes. The amphiphilic complexes utilized for the experiments (**26**–**28** lanthanide complexes, see Table 2), were previously proposed by Lattuada et al. as a new class of stable blood pool MRI/MRA contrast agents after incorporation in mixed aggregates [108,109]. The incorporation in DPPC-based liposomes of La-**26** complex, bearing two saturated C18 chains, did not affect so much the water permeability of the membrane, while the incorporation of La-**27** complex, bearing one saturated C12 chain for each coordination arm of the chelate, significantly accelerated the water mobility across the membrane. This result suggests the incorporation modality adopted by the latter amphiphile destabilizes the compact packing of the DPPC bilayer. Instead, when the amphiphilic complexes (**26** and **28** complexes) are incorporated in unsaturated liposomes (POPC-based liposomes) a stabilization of the aggregate occurs and the water permeability of the membrane decreases proportionally to the amount of the incorporated compound [110]. Another extremely important parameter influencing the relaxivity is represented by the transition phase temperature. Liposome bilayer, which presents a liquid-crystalline state have a high water exchange rate between the interior and exterior liposome comparments, allowing bulk water to experience magnetic interaction with the Gd-chelates located on the inner surface. On the contrary, liposome bilayer in the solid–gel state have a low water exchange rate, making the inner surface chelates less accessible for the bulk water and thereby decreasing their contribution to the overall relaxivity [77]. On the other hand, the lateral motion on the liposome surface is about twice as high in

a liquid-crystalline membrane compared to a gel state membrane [111]. This should give rise to a longer $^{***}\tau_R$ for the Gd-chelates incorporated into a gel state-membrane with respect to complexes incorporated in liquid-crystalline state, thereby increasing their relaxivity.

The cholesterol introduction in the formulation has always a positive effect on the relaxivity. The influence of cholesterol on the liposome membrane is associated to the phase transition temperature of the latter. With the incorporation of cholesterol into a solid–gel liposome fluidises the membrane, leading to increased transmembrane water permeability and hence an increased relaxivity of the Gd-chelates present inside the liposomes. In the liquid-crystalline liposomes the positive effect observed upon cholesterol incorporation is most likely related to an increase in the membrane rigidity. The rotational correlation time (τ_R) of the Gd-chelate is prolonged, without affecting adversely the conditions of fast water exchange. According to these considerations, the highest relaxivity was obtained for DMPC-based liposomes (24–42 $mM^{-1}\,s^{-1}$) compared to the DSPC-ones (20–28 $mM^{-1}\,s^{-1}$). According to Gløgård assumption, Strijkers et al., verified that unsaturated-based liposomes (DOPC/DSPE-PEG2000/Gd-DTPABSA) have higher relaxivity with respect to the saturated-based ones (DSPC/DSPE-PEG2000/Gd-DTPABOA), and the adding of cholesterol to the liposome formulation leads to a further, although smaller, increase of the relaxivity [112].

Moreover, Aime et al. [113], proposed systems based mixed liposomes in which gadolinium complexes are conjugated to phospholipids by a disulfide bond, that is sensitive to radical presence: when the disulfide bond is cleaved upon radical attach the T_1-relaxivity of the system decreases to approach the value for the free Gd chelate.

Nowadays, the research is devoted to find new multifunctional liposomes, able to address at the main time two or more objectives, such as pDNA transfection or diagnosis and treatment of diseases. For example, in the last year Miller et al. reported the utility of liposomes as bimodal paramagnetic and fluorescent imaging systems both for *in vitro* cell labelling and *in vivo* tumour imaging [114]. They synthesized the amphiphilic gadolinium complex Gd-DOTA·DSA (compound **28** in Table 2) and incorporating it in DOPC/Chol/DSPE-PEG_{2000} liposomes. A small amount of the fluorescent lipid DOPE-Rhodamine (0.5–1.0 mole%) was also incorporated in the liposome formulation in order to obtain fluorescent aggregates. This method permits to quantify uptake and internalization processes of liposomes into the cell cytosol. Liposomal surface was modified with PEG to prolong presence of contrast liposomes in the body [115]. In fact, surface modification with polymers produces changes in biodistribution and body retention of liposomes [116]. In greater detail, modification with PEG is known to prolong the circulation times upon intravenous administration of the coated liposomes [117] this is due to the prevention of the liposomes opsonisation with macrophage-recognizable [118]. Liposome formulation was intravenously injected in nude mice in which IGROV-1 (human ovarian cancer cells) xenografts were previously implanted. Post i.v. injection of Gd-liposomes, xenograft tumours were monitored by MRI over a 24 h period. Over this period, a substantial 60% reduction in tumour T_1 values compared to the situation with control liposomes (without Gd) and visibly enhanced tumour image brightness. This outcome suggested that liposomal half-life time ($t_{1/2} > 4$ h) is long enough to allow passive targeting to the xenograft tumour by an enhanced permeation and retention (EPR) mechanism due to the porous nature of the endothelial cell layer [119]. The fluorescence imaging of tumour tissue slices (post-mortem) supported liposome accumulation in intravascular spaces and in surrounding viable tumour tissue.

4.3. Micelles of amphiphilic poly(gadolinium complexes) polymers

Polymeric micelles can be obtained by self-assembling block-copolymers consisting of hydrophilic and hydrophobic monomer units with the length of the hydrophilic block exceeding to some extent that of the hydrophobic one. If the hydrophilic block length is high, copolymers exist in water as individual molecules, while copolymers with very long hydrophobic block form lamellar structures [120]. In different amphiphilic polymers, monomer units with different hydrophobicity can be arranged into two conjugated blocks each consisting of monomers of the same type (A–B-type copolymers), or can form alternating blocks with different hydrophobicity (A–B–A-type copolymers). The hydrophilic copolymers can also represent a backbone chain to which hydrophobic blocks are attached as side chains (graft copolymers). Polymeric micelles have recently attracted much attention as contrast agents in MRI for their more stability with respect to micelles prepared from conventional surfactants. Usually, amphiphilic micelle-forming monomers include PEG blocks (1–15 kDa) as hydrophilic corona forming blocks [121] for its low toxicity and its capability of shield micelles from biologically active macromolecules [122]. At the same time, a variety of monomers may be used to build hydrophobic core-forming blocks: propylene oxide [123], L-lysine [124], aspartic acid [125], β-benzoyl-L-aspartate [126], γ-benzyl-L-glutamate [127], spermine [128], and some others. Some of these hydrophobic-forming blocks such as poly(lysine) and poly(aspartic acid) are largely employed in the synthesis of copolymers as MRI contrast agents for the presence of reactive functions on their side chains for the coupling of chelating agents. Anyway, only few examples of supramolecolar aggregates obtained by using gadolinium-containing copolymers are reported as MRI contrast agents: compounds **30**–**33** in Table 3. The low number of proposed compounds yields difficult to take an appropriate survey of the relationship between their structures and relaxivities.

An example is represented by the poly(lysine)-based polychelating polymer (Gd-DTPA-PLL-NGPE) (compound **30**, Table 3) proposed by Torchilin et al. in 2000 [115,129]. Gd-DTPA-PLL-NGPE polymer, an A–B-type copolymer, can be easily incorporated into liposome membranes by the presence of a phospholipid residue (NGPE) at one end of the molecule. Each polymeric DTPA-PLL-NGPE moiety complex about six Gd(III) ions (at least 31% w/w) and is incorporated in egg lecithin liposomes. The presence of a single-terminus modified polymer containing multiple chelating groups permits to increase the quantity of the carrier-associated reporter metals, thus increasing the contrast-to-lipid ratio and enhancing the signal intensity at the same quantity of the liposomal carrier. Upon subcutaneous administration, liposomes penetrate the lymphatics and effectively visualize its elements in corresponding imaging modalities. Liposomes mostly stay within lymph fluid rather than accumulate in the nodal macrophages (because of protective effect of surface PEG fragments) and rapidly move via the lymphatic pathway. They can serve as fast and efficient lymphangiographic agents for scintigraphy or MR imaging. Relaxivity behaviour and the resistance to the phagocytic cells of chelating polymer-bearing liposomes were improved by incorporation of amphiphilic PEG into the liposome membrane.

Successively, Yokoyama et al. designed and developed polymeric micelles of cationic polymers (polyallylamine or protamine) and several anionic block A–B-type copolymers (PEG_x-$P(Asp)_y$) that bound Gd(III). Polymeric micelles are able to increase the signal intensity at the targeted site and to lower, at the same time, the signal intensity in the vasculature space. In fact it is well known that high concentration of the contrast agent in the vasculature space creates a disadvantageous background, since blood

Table 3
Relaxivity values, r_1, at 20 MHz and 25 °C, of polymeric aggregates.

Prinicipal investigator and reference	Compound name	#	Schematic representation of amphiphilic gadolinium complexes	r_1 (mM^{-1} s^{-1})
V.P. Torchilin [115,129]	Gd-DTPA-PLL-NGPE	**30**	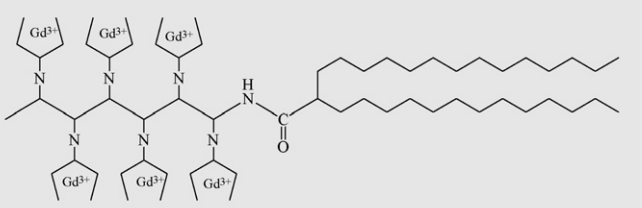	[a]
M. Yokoyama [130]	PEG_x-P(Asp_y(DTPA-Gd)$_z$)	**31**	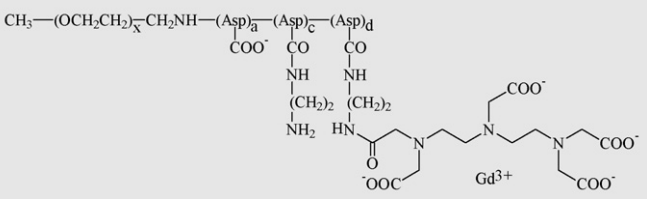	10–11
S.H. Cho [131]	PSI-mPEG-C16-DTPA(Gd)	**32**	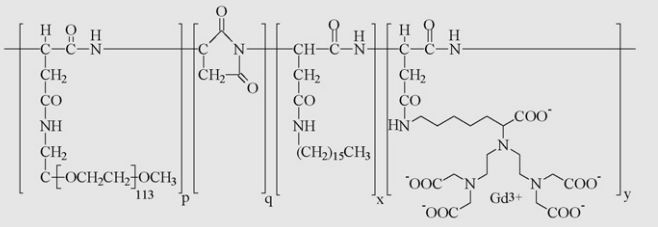	[b]
K.L. Wooley [132]	PAA_{52}-b-PMA_{128}-DTPA(Gd)	**33**	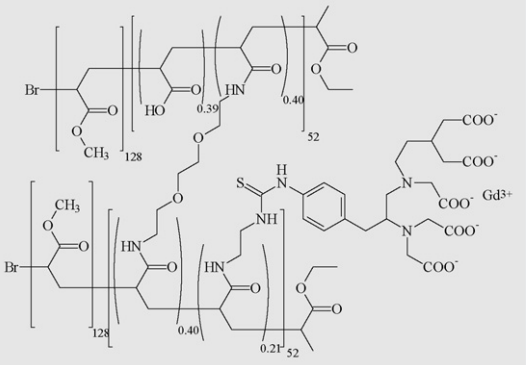	21.2

[a] Relaxivity values reported as function of liposomal lipid concentration, see Ref. [115].
[b] Value not reported.

is supplied both to targeted tissues (or organs) and to non-target ones. PEG_x-P(Asp_y(DTPA-Gd)$_z$) **31** polymer was obtained by coupling of the DTPA(Gd) complexes on the anionic core-forming block poly(aspartic acid), previously modified by the introduction of an ethylenediamine group [130]. This polymeric micelle-type MRI contrast agent changes relaxivity upon micelle formation and desgregation: Gd(III)-binding block copolymer alone showed high relaxivity values from 10 to 11 mM^{-1} s^{-1}, while polymeric micelles exhibited low relaxivity values from 2.1 to 3.6 mM^{-1} s^{-1}. The different relaxivity values can be ascribed to the different exposition to the water of the Gd(III) complexes in the two macromolecular systems. In polymeric micelles Gd(III) complexes are less accessible to water molecules because of their location in the inner core of the micelles.

Another example of polymeric micelle-type MRI contrast agent was proposed by Cho et al. Aggregates were obtained by self-assembling of PSI-mPEG-C16-(DTPA-Gd), (see Table 3, compound **32**) a A–B–A-type polymeric compound prepared by conjugating a hydrophilic methoxy-poly(ethylene glycol) (mPEG), a hydrophobic group (C16) and a gadolinium complex (DTPA-Gd) to a biodegradable polymer (PSI). *In vitro*, the prepared micelles showed the enhancement of MRI contrast over five times of commercially available Omniscan® [131].

Alternatively to the polymeric aggregates above reported, obtained by self-assembling of polychelating polymers, Turner et al. proposed a procedure in which gadolinium complexes are covalently bound on the external surface of the polymeric aggregate only after the assembling process. The authors developed shell-crosslinked knedel-like nanoparticles (SCKs) as the scaffolding from which to produce contrast-enhancing agents. SCKs are self-assembled core–shell materials, originating from amphiphilic block copolymer micelles that are covalently stabilized by a crosslinking reaction. The SCKs were prepared from the aqueous assembly of a diblock copolymer, PAA_{52}-*b*-PMA_{128}, and crosslinking the resultant micellar structure throughout the shell layer [132]. After the assembling, PAA_{52}-*b*-PMA_{128}-DTPA(Gd), **33** was obtained by

functionalizing SCK nanoparticles by DTPA chelating agent. Hydrodynamic diameter and aggregation number of amphiphilic block copolymer chains per SCK were 40 nm and 160, respectively. Although the low yield of functionalization reaction (21% and 510 Gd(III) complexes per nanoparticles), due to the steric hindrance of the two reactants, the relaxivity value per SCK nanoparticle was of 10,800 at 25 °C (21.2 mM^{-1} s^{-1} per Gd ion).

5. Supramolecular aggregates derivatized with peptides or antibodies as target selective MRI contrast agents

All the above reported micelles and liposomes have been developed with the aim to increase the relaxivity of each gadolinium atom present in the supramolecular aggregates; moreover the high number of gadolinium complexes for each aggregate enhances the contrast efficacy of these systems, that are also characterized by peculiar pharmacokinetic properties and biodistribution behaviour. Anyway, a challenge in diagnosis is the non-invasive detection of molecular markers of diseases in order to identify and visualize them in an early stage and to be able to follow the effect of therapy. Specific information on molecular markers can be obtained with the use of targeted contrast agents, which are directed to a molecular entity of interest, e.g. endothelial cells surface receptors that are overexpressed as a consequence of a disease process. The labelling of gadolinium-containing micelles and liposomes with bioactive molecules such as antibodies and peptides combines together the high relaxivity of the supramolecular aggregate with the target selectivity due to the presence of the bioactive moiety. Several gadolinium-based supramolecular aggregates derivatized with peptides or antibodies are also modified with the introduction of a fluorescent probe to have a bi-modal detection system and thus confirming their *in vitro* target selectivity by fluorescence techniques. Different synthetic procedures have been developed to introduce the bioactive molecule on the external surface of the supramolecular aggregate [62]. The choice of synthetic strategy depends on whether coupling is performed before or after assembly of the supramolecular aggregate. The obvious goal of each approach is to achieve high coupling efficiency, but with the ligand retaining full binding affinity for its target receptor. The coupling of a ligand after the aggregate has been assembled involves the introduction of suitable activated functional groups onto the terminus of one of the aggregate components. Activated functional groups must be compatible with the aggregation process and should remain available on the aggregate surface for efficient chemical ligation of the bioactive ligand. As schematized in Fig. 5a, an example of this approach consists in the preparation of liposomes or micelles containing a DSPE-PEG monomer derivatized with a N-maleimido function on the distal end of the DSPE-PEG monomer; after aggregate formation the externally exposed N-maleimido function reacts with the bioactive molecule, according to the sulphydryl-maleimide coupling method, to give the labelled supramolecular aggregate. Another example with this approach is based on the obtainment of biotinylated aggregates using a biotinylated liphophilic monomer in the surfactant mixture; in a two-steps process the biotinylated supramolecular aggregates react with avidin and then with the biotinylated peptide or antibody giving a non-covalently labelled compound (Fig. 5b). This strategy has proven to be particularly successful for the coupling of large ligands such as monoclonal antibodies.

The coupling of a bioactive ligand to an aggregate component before aggregation is, in principle, chemically less complicate, but has the disadvantage that, at least in the case of liposomes, following final assembly of the aggregate a fraction of the conjugated bioactive ligand remains entrapped in the interior region and is not more available for receptor binding. This labelling procedure, based on the use of amphiphilic peptides that assemble together with amphiphilic gadolinium complexes in the peptide labelled supramolecular aggregates, is schematized in Fig. 5c.

In this chapter, micelles and liposomes based on lipophilic gadolinium complexes and externally derivatized with antibodies and peptides acting as target-specific contrast agents in MRI will be described.

5.1. Supramolecular aggregates based on lipophilic gadolinium complexes and derivatized with antibodies

As stated above, liposomes have been studied extensively during the last two decades as drug carrier vehicles. For this purpose, they have been optimized in terms of their stability, circulation time *in vivo*, and membrane composition. Liposomes are based on biocompatible natural or synthetic amphiphilic lipids, they can be sized to a defined diameter in the range of 50–500 nm, and can also be coated with polymers to increase their stability and prolong their *in vivo* half-life. Mulder et al. [29] developed pegylated paramagnetic liposomes, immuno-liposomes, composed by Gd-DTPA-bis(stearylamide), cholesterol, DOPC and N-maleimide-DSPE-PEG2000 phospholipids, and derivatized with antibody molecules coupled to the distal end of the PEG chains. The chosen antibody is able to detect E-selectin expression on human umbilical vein endothelial cells, this is an attractive model for receptor expression on endothelial cells, since E-selectin level can be regulated by TNFα and represents a model system for a variety of endothelial cell surface receptors that are of physiological and therapeutic interest, including αvβ3 integrins and VEGF receptors. *In vitro* MRI experiments on pellets gave excellent results in terms of selectivity: the T_1-weighted image of pellets containing 10^6 TNFα treated human umbilical vein endothelial cells, incubated with the E-selectinAB-liposomes had a much higher signal intensity than that of control systems, due to a large shortening of T_1 in this system.

The same authors described, very recently, the use of pegylated, fluorescent and paramagnetic micelles (immuno-micelles) for imaging of macrophages in atherosclerotic plaques [133]. Micelles were obtained by combining together Gd-DTPA-BC18, DSPE-PEG2000 and N-maleimide-DSPE-PEG2000 phospholipids; macrophage scavenger receptor (MSR)-specific antibodies were conjugated to micelles through N-maleimide function. The abdominal aortas of atherosclerotic apolipoprotein E knockout (apoE-KO) mice were imaged with T_1-weighted high-resolution MRI before and 24 h after intravenous administration of the micellar contrast agent. Pronounced signal enhancement was observed for apoE-KO mice that were injected with MSR-targeted micelles, while the aortic vessel wall of mice injected with non-targeted micelles showed little signal enhancement, thus demonstrating that macrophages in apo-E-KO mice can be effectively and specifically detected by MRI upon administration of a pegylated micellar gadolinium contrast agent.

A different approach in preparing immuno-micelles was used by the same authors [92,134–137]: they obtained mixed micelles combining the amphiphilic gadolinium complex, Gd-DOTA-C16, the POPC phospholipids and the Tween 80 surfactant, moreover a little amount of DPPE-biotin was added to have biotinylated micelles. Immuno-micelles are obtained by adding, first, a specific amount of avidin to the biotinylated micelles and, then, the biotinylated antibodies. Micelles were characterized for their size (80–90 nm) their relaxivity (25–33 mM^{-1} s^{-1} per Gd ion) and number of gadolinium atoms (3500–4000). They were used for *ex vivo* images [134] and *in vivo* experiments [135] to detect atherosclerosis, targeting macrophage scavenger receptors. Both studies confirmed that this kind of immuno-micelles provides excellent validated *in vivo* enhancement of atherosclerotic plaques. The enhancement seen is related to macrophage content of the atherosclerotic vessel area

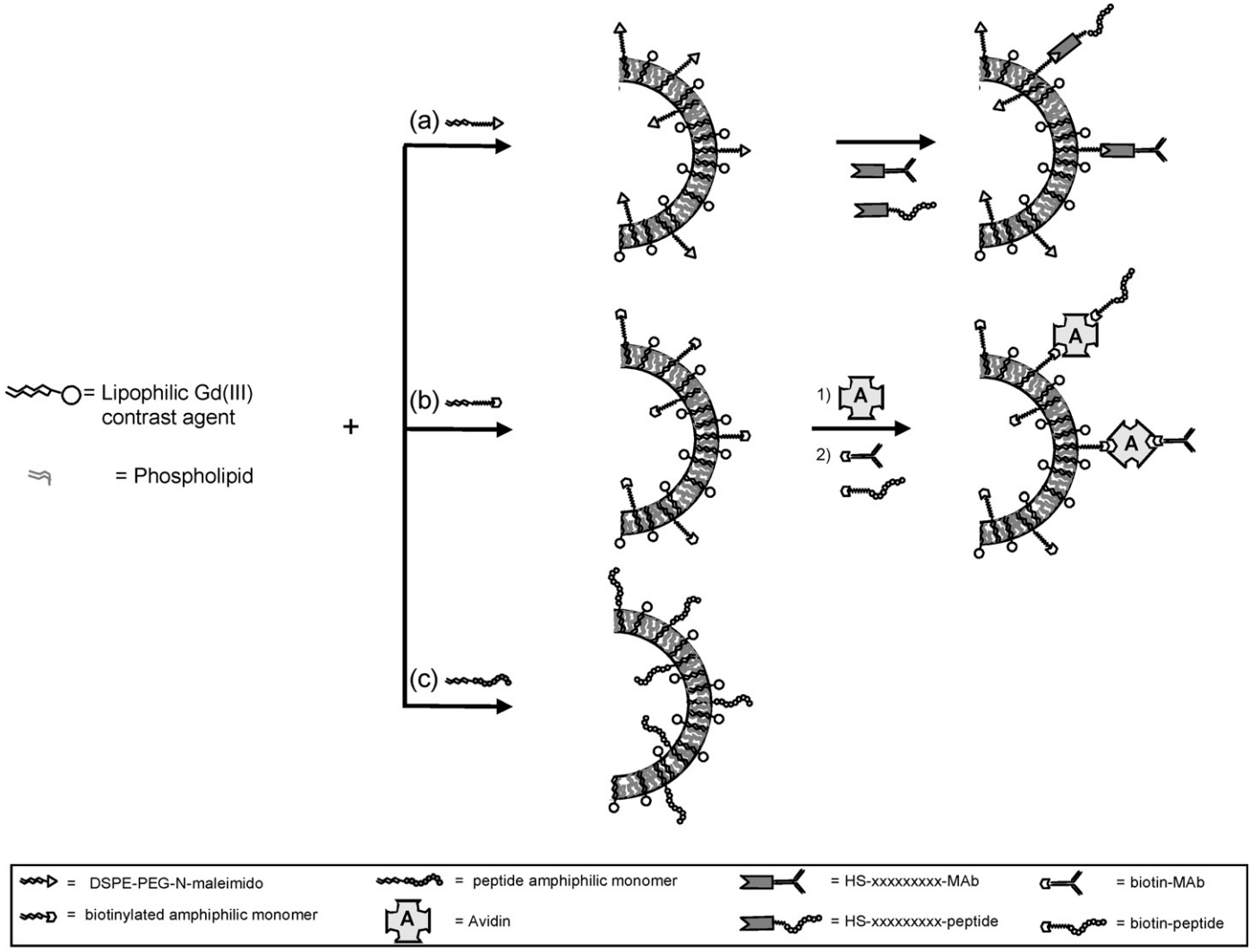

Fig. 5. Examples of labelling procedures to introduce the bioactive molecule on the external surface of supramolecular aggregates: according to the first procedure (a), a DSPE-PEG monomer derivatized with a N-maleimido function is incorporated in the mixed aggregate; after aggregate formation the externally exposed N-maleimido function reacts with the bioactive molecule to give the labelled supramolecular aggregate. In another approach (b) biotinylated aggregates are obtained by using in the surfactant mixture a biotin bearing lipophilic tail; successively, in a two-steps process, the biotinylated supramolecular aggregates react with the protein avidin, then biotinylated peptides or antibodies interact in free avidin sites giving a non-covalently labelled compound. In the last case, (c) labelled aggregates are obtained assembling a mixture solution of amphiphilic peptides and amphiphilic gadolinium complexes.

imaged, as clearly reported in Fig. 6, thus these immuno-micelles may aid in detection, by MRI, of high macrophage content associated with vulnerable plaque.

The same approach based on biotin–avidin affinity interaction has been used by Li and co-workers in their pioneering work on immuno-liposomes. They prepared polymerized vesicles of 300–50 nm in diameter by UV irradiation of a mixture of Gadolinium-DTPA polymerizable lipid, a polymerizable biotinilated lipid and diacetylene phosphatidilcholine filler lipid [92,136,137], then derivatized the liposomes with a specific antibody. Very interesting results have been obtained for *in vivo* detection of tumour angiogenesis targeting the integrin αvβ3 [137]. They used polymerized liposomes derivatized with the LM609 monoclonal antibody able to target endothelial αvβ3. As shown in Fig. 7, this approach provides enhanced and detailed imaging of rabbit carcinomas by directly targeting the gadolinium based contrast agent to the angiogenic vasculature. In addition, angiogenic "hot spots" not seen by standard MRI were detected.

Similar antibody conjugated paramagnetic polymerized liposomes were used to target the intercellular adhesion molecule-1, an endothelial leukocyte receptor on cerebral microvasculature in experimental autoimmune encephalitis [138]. High-resolution MRI of mouse brains *ex vivo* demonstrated that antibody conjugated gadolinium based liposomes binding conferred significant enhancement of signal intensity as compared to control images.

5.2. Supramolecular aggregates based on lipophilic gadolinium complexes and derivatized with peptides

Gadolinium-based paramagnetic supramolecular aggregates derivatized with bioactive peptides have been essentially developed in order to have selective contrast agents capable of visualizing neovascularization and angiogenic processes targeting αvβ3 integrins or tumour proliferization and metastasis targeting cellular receptors that are overexpressed by cancer cells. Some interesting supramolecular constructs were initially developed by Stupp and co-workers [30,139] by self-assembly of amphiphile peptide molecules carrying a DOTA–gadolinium complex. They synthesized, by solid-phase technique peptide amphiphilic molecules containing the RGD peptide sequences, important for cell adhesion,

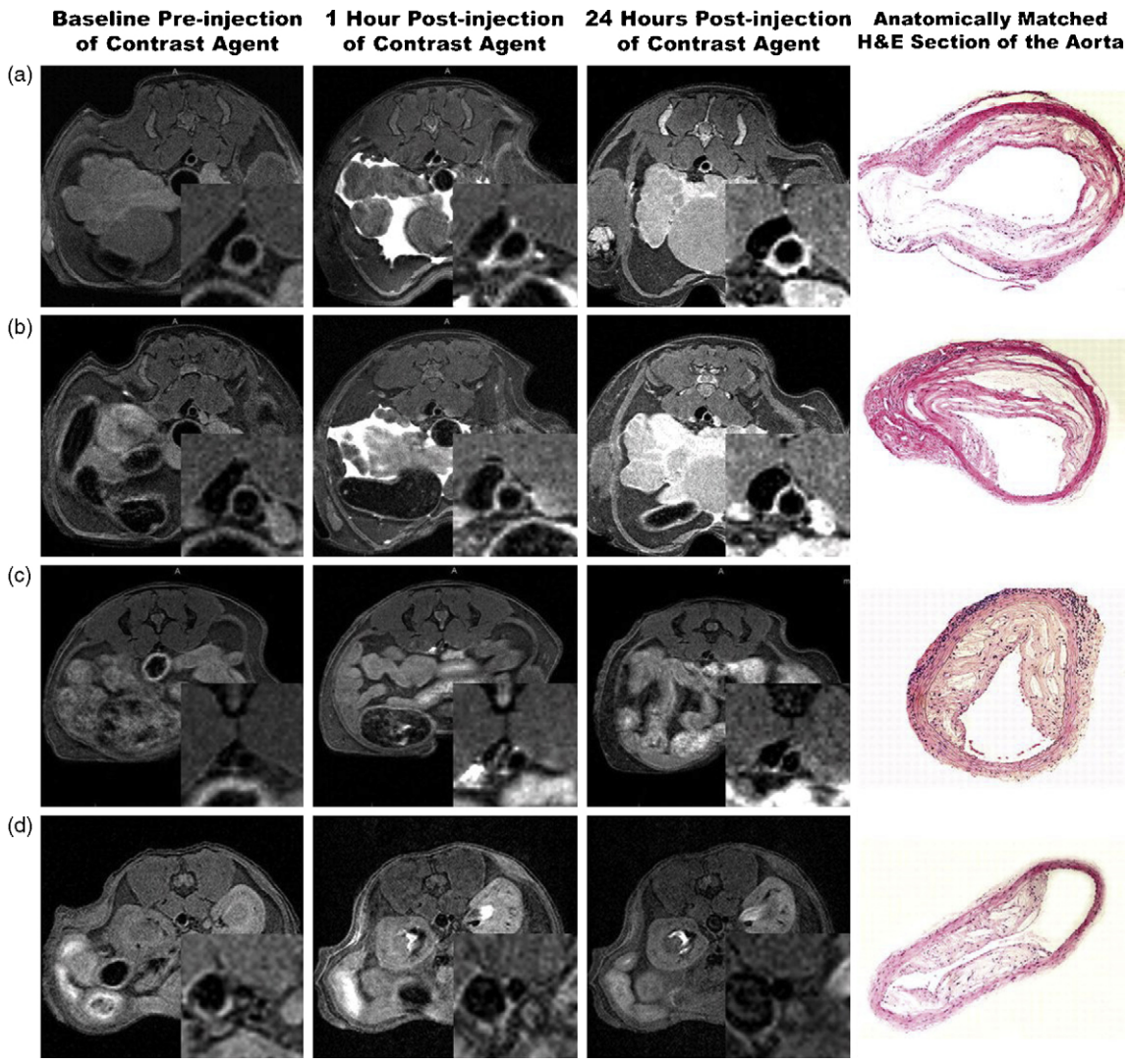

Fig. 6. *In vivo* MRI images obtained at baseline and postinjection of macrophage-targeted immuno-micelles (a and b), untargeted micelles (c), and Gd-DTPA (d) in ApoE$^{-/-}$ mice. The MRI insets are enlargements of the aortas. (a–d) Right show H&E sections of the aorta at the identical anatomic level as the MRI images from the same animal [135]. Reproduced by permission of PNAS.

or a cysteine rich peptide sequence for cross linking of the self-assembled systems, and a DOTA-Gd complex covalently bound to the N-terminus of the peptide. These amphiphilic molecules self-assemble into spherical and fiber-like nanostructures, that show an enhanced T_1 relaxation time with a relaxivity increased up to 22.8 mM^{-1} s^{-1} after assembling in supramolecular aggregates [30]. Moreover, van Tilborg recently developed lipid-based bimodal contrast agents that enable the detection of apoptotic cells, by functionalizing liposomes with the apoptosis target protein Annexin-5 [140].

In next sections we will review supramolecular aggregates derivatized with RGD peptides or similar sequences capable of targeting αvβ3 integrins and aggregates derivatized with the CCK8 bioactive peptide capable of targeting cholecystokinin receptors overexpressed on cancer cell membranes.

5.2.1. Gadolinium-based paramagnetic supramolecular aggregates for selective targeting of tumour angiogenesis

The αvβ3 integrin represents an attractive target for molecular imaging of tumour angiogenesis because its expression is dramatically increased on neovasculature but is not generally expressed on quiescent endothelial cells. Schmieder et al. [141] prepared nanoparticles assembling together perfluorooctyl-bromide (PFOB), a surfactant mixture, the lipophilic gadolinium complex Gd-DTPA-bisoleate, and a little amount of MPB-PEG2000-DSPE; the nanoparticles were derivatized by conjugating a thiolated peptidomimetic vitronectin antagonist to the maleimidophenyl function of MPB-PEG2000-DSPE. The nanoparticles of approximately 270 nm in diameter, containing ≈300 homing ligands on their surface and 90,000 Gd ions for particle showed a relaxivity of about 20 mM^{-1} s^{-1} per each gadolinium atom. These nanoparticles were used to detect and characterize angiogenesis of developing melanoma xenografts in nude mice (Fig. 8), confirming the usefulness of the paramagnetic and target selective nanoparticles in visualization of very small tumours (≈30 mm^3) by increasing spatial resolution and using a small surface coil. Similar liposomes, conjugated with the αvβ3-specific RGD peptide attached to PEG moieties, have been developed by Mulder et al. [119,142]. These liposomes were used as MRI contrast agents in *in vitro* and *in vivo* studies for detection of αvβ3-integrin and visualization of proliferating human activated endothelium tumour. *In vitro* studies demonstrate that RGD-liposomes associate impressively with proliferating endothelial cells associated with cancer, they are internalized by the cells and localized to a perinuclear compartment. *In vivo* studies indicate that RGD-liposomes are localized at the rim of the tumour with a distribution pattern that closely correlates

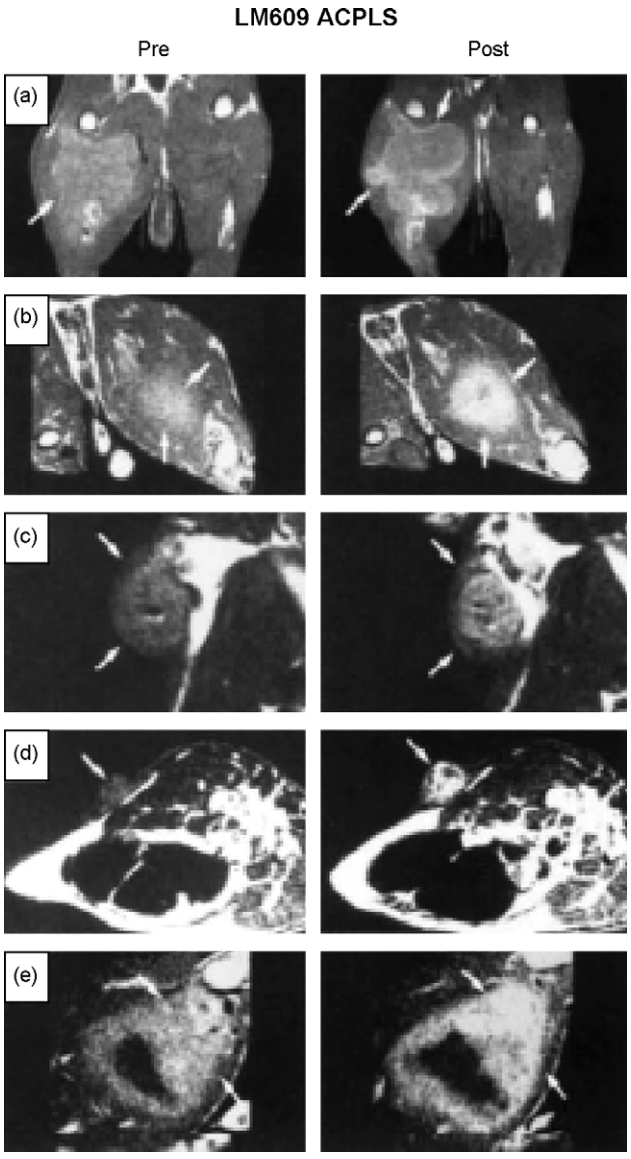

Fig. 7. Anti-αvβ3 (LM609) ACPLs confer T1-weighted (T1W) MR signal enhancement of rabbit tumours. (a–e) T1W images of rabbit pre-and 24 h post-targeted contrast administration. Arrows indicate tumours. (a) Coronal images of rabbit-bearing tumour in the right thigh muscle. 24 h following LM 609 ACPL administration, the tumour periphery (arrows), an area of active angiogenesis and αvβ3 expression (see Fig. 2a), is clearly demarcated. (b) Axial images show a poorly visible intramuscular tumour pre-contrast. Subsequent to LM609 ACPL administration, the tumour is more readily discerned. (c) Coronal images of a rabbit with V2 carcinoma implanted subcutaneously. Tumour cannot be distinguished from surrounding normal skin pre-contrast. However, distinct tissue margins are apparent post-contrast. (d) LM609 ACPLs improve visualization of a subcutaneous tumour. Hypointense areas represent necrotic tissue (no blood supply). (e) An axial pre-contrast image shows a hyperintense intramuscular tumour with central necrosis. Post-contrast, LM609 ACPLs reveal angiogenic "hot spots" within viable tumour [137]. Reproduced by permission of Nature Medicine.

with the position of angiogenic blood vessels in the tumour, which are found mainly at the rim. Moreover these nanoparticles can be used, by MRI techniques, to non-invasively measure the efficacy of angiogenesis inhibitors during the course of a therapy [142].

Griffioen co-workers used Anginex, a synthetic 33-mer angiostatic peptide that is capable of homing to activated endothelium, as targeting ligand [143]. Paramagnetic liposomes obtained by co-aggregation of Gd-DTPA-BC18, maleimide-PEG2000-DSPE, DSPC and cholesterol, were derivatized with Anginex by covalently attaching the synthetic peptide by sulphydryl-maleimide coupling

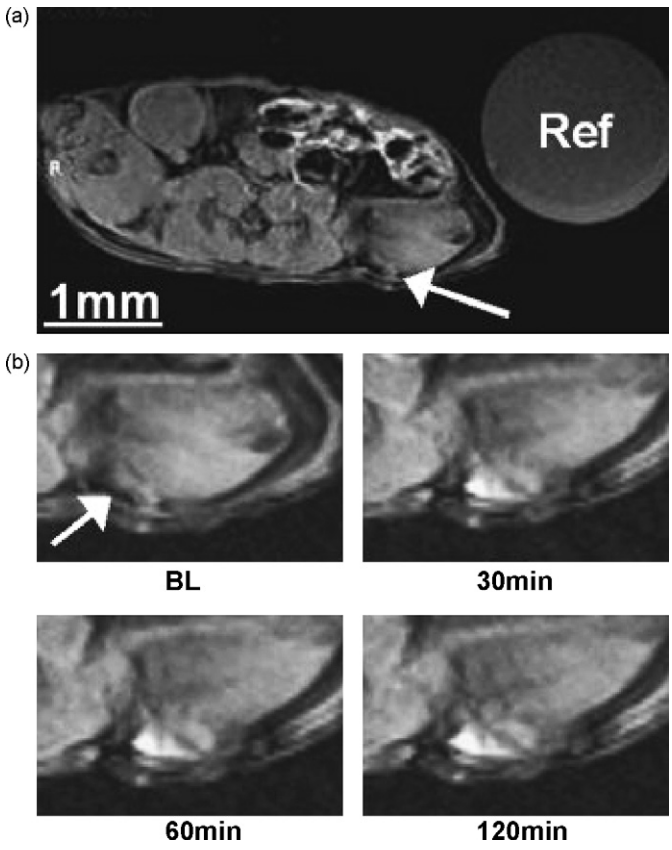

Fig. 8. (a) T1-weight MR image (axial view) of an athymic nude mouse before injection of paramagnetic αvβ3-targeted nanoparticles. Arrow indicates a C32 tumour that is difficult to detect (Ref.-Gd in 10 cc syringe). (b) Enlarger section of an MR image showing T1-weight signal enhancement of angiogenic vasculature of early tumours over 2 h as detected by αvβ3-targeted paramagnetic nanoparticles (BL = baseline image) [141]. Copyright (2005, John Wiley & Sons, Inc.). Reprinted with permission of Wiley-Liss, Inc., a subsidiary of John Wiley & Sons, Inc.

to maleimide-PEG-DSPE and studied *in vitro* on cell cultures and by MRI of cell pellets. The results indicate that the angiostatic peptide Anginex is a potent ligand for the targeting of paramagnetic liposomes to activated endothelial cells; in addition the *in vitro* results showed a high specificity of the anginex-conjugated paramagnetic liposomes for endhotelial cells that was confirmed by MRI.

A different approach was used by Mulder et al. [144] that developed MRI detectable and targeted quantum dots. Quantum dots were coated with paramagnetic and pegylated lipids, which resulted in a relaxivity, r_1, of nearly 2000 $mM^{-1}\,s^{-1}$ per quantum dot. The quantum dots were functionalized by covalently linking αvβ3-specific RGD peptides, and the specificity was assessed and confirmed on cultured endhothelial cells. For their high relaxivity and target specificity these constructs seem excellent contrast agents for molecular imaging of tumour angiogenesis. Polymeric constructs have been developed by Ke et al. [145]. They prepared cyclic RGDdFK target poly(L-glutamic acid)-(Gd-DO3A) conjugate with a biodegradable cystamine spacer, and evaluated these construct for *in vivo* detection the angiogenic biomarker αvβ3-integrin in neoplastic tissues with T_1 mapping by MRI. The targeted conjugate showed high specific binding to human prostate carcinoma cells with a significant decrease of T_1 values.

5.2.2. Gadolinium-based paramagnetic supramolecular aggregates derivatized with CCK8 bioactive peptide

Several supramolecular aggregates derivatized with the CCK8 bioactive peptide on their surface have been developed by Morelli and Paduano [92,146–149]. Most of these systems have been

obtained by co-assembling two amphiphilic monomers, one containing the gadolinium complex and the other the bioactive peptide CCK8. The presence in the aggregates of two separated monomers allows the tuning of the ratio between the active components in order to find the right compromise between the number of peptide targeting molecules on the aggregate surface, and of the gadolinium-chelate complexes. The peptide sequence (Asp-Tyr-Met-Gly-Trp-Met-Asp-Phe-amide, CCK26-33 or CCK8) corresponds to the C-terminal fragment of the cholecystokinin hormone and provides the binding sequence for the cholecystokinin receptor subtypes A and B (CCK_A-R and CCK_B-R) [150]. Overexpression of both of these receptor subtypes has been demonstrated in certain human tumours: CCK_A-R is overexpressed in pancreatic cancer, and CCKB-R has been found in small cell lung cancer, colon and gastric cancers, medullary thyroid carcinomas, astrocitomas and stromal ovarian tumours [151].

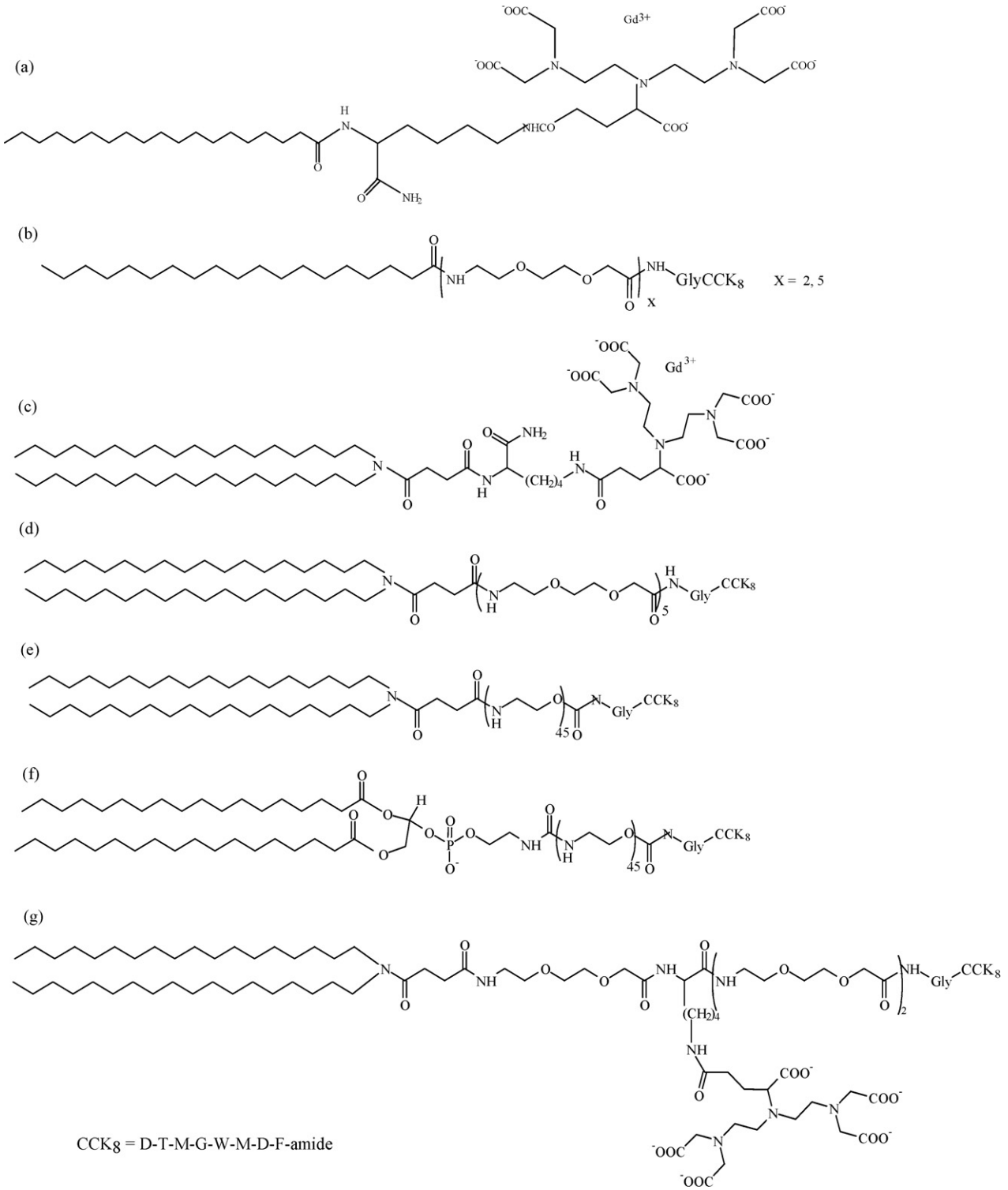

Fig. 9. Schematic representation of amphiphilic monomers used to prepare supramolecular aggregates derivatized with CCK8 bioactive peptides and DTPAGlu(Gd) complexes. The amino acid sequence of CCK8 peptide is reported by using the one-letter amino acid code.

The design of the molecules has been developed with the main aim to realize supramolecular aggregates (micelles or liposomes) suitable for *in vivo* use as target selective contrast agents: low cmc values of the aggregates in physiological environment, no toxicity of the entire aggregate and of the single monomers, and availability of the bioactive peptide adequately exposed above the surface. To achieve this goal the design has been gradually upgraded. In the first attempt single-tailed amphiphilic monomers (C18DTPAGlu(Gd) and C18L*x*CCK8, L = 8-amino-3,6-dioxaoctanoic acid, $x = 2$, 5) reported in Fig. 9 (compounds **a** and **b**) were prepared. An extensive characterization of these aggregates, with or without complexed Gd(III) ions, has been reported. The monomers give mixed spherical micelles with aggregation number around 60–65, and a radius of approximately 40 Å. The peptide seems well exposed on the micelle surface, particularly in the case of compounds with L5 linker, and, as expected, the relaxivity value is in the 18–19 $mM^{-1}\,s^{-1}$ range. Unfortunately the aggregate stability, indicated by the cmc values, was not high enough to guarantee integrity following dilution, such as after intravenous injection for the intended *in vivo* use. To overcome these problems, new mixed supramolecular adducts in which both the amphiphilic monomers (second generation monomers) contain as lipophilic tail, a moiety with two hydrophobic C18 chains were prepared [92]. The two hydrocarbon tails on the same monomer allow formation of very stable aggregates. Moreover monomers bearing two hydrophobic tails, do not present hemolytic effects and toxicity for their higher similarity with membrane phospholipids with respect to single chain amphiphiles [108]. The aggregates obtained by assembling the two lipophilic monomers $(C18)_2$DTPAGlu(Gd) and $(C18)_2$L5CCK8 in 70:30 ratio (Fig. 9, compounds **c** and **d**), are characterized by the presence of bilayer structures (open bilayers and liposomes) under conditions of physiologic ionic strength. The relaxivity value of each gadolinium complex in liposomes (hydrodynamic radius of about 300 Å) was of ∼21.0 $mM^{-1}\,s^{-1}$. Both the complex in the inner and in the outer layer contribute to the observed paramagnetic relaxation rate, because of the high membrane water permeability due to the high number of negative charges (two per each DTPAGlu(Gd) complex) in the aggregate.

Similar results have been obtained for aggregates in which $(C18)_2$L5CCK8 monomer was replaced by $(C18)_2$PEG2000CCK8 one (Fig. 9, compound **e**) [152]. In this case, to obtain adequate distancing of the bioactive peptide from the surface of the supramolecular aggregate, and reduce potential hindrance to its specific binding activity, a larger hydrophilic spacer is introduced between the peptide N-terminus and the lipophilic tails. Due to its size and the well-known empathy for water, poly(ethyleneglycol) (PEG_{2000} MW = 2000) has been used. The supramolecular aggregated, obtained by mixing togheter the two monomers in 70:30 ratio and performing sonication and extrusion steps, are characterized by rod-like micelles and closed vesicles. From the structural point of view, PEG-containing monomers showed lower tendency to form liposomes in comparison to L5-containing monomers, also after sonication and extrusion processes.

The authors also reported a study in which the structure of the supramolecular aggregates [148] is influenced by the ratio between the two monomers. Bilayer structures are obtained in the case of samples containing only DSPE-PEG_{2000}-CCK8 (Fig. 9, compound **f**), or a quantity of $(C18)_2$DTPAGlu(Gd) up to 50%. This is probably driven by the high energy transferred to the system by extrusion and sonication procedures. By increasing the amount of $(C18)_2$DTPAGlu(Gd) in the aggregate, a bilayer–rod-like micelle transition is observed. The proton relaxivity resulted to be exactly the same (17.2 $mM^{-1}\,s^{-1}$) for both open bilayers and rod-like micelles though in the two cases its value is the result of the combination of different local and global contributions.

Many of the above-described systems have also been characterized *in vitro* and *in vivo* for their selective binding activity. For this pourpose the gadolinium atom is replaced with gamma emitting radioisotope ^{111}In and the aggregate targeting and biodistribution is studied by nuclear medicine experiments. Biological tests show properties that appear potentially suitable for clinical applications: (i) significantly higher concentration of aggregates in receptor expressing xenografts relative to controls has been established *in vivo*, suggesting that these aggregates may be utilized to increase concentration of the gadolinium contrast agent to tissues expressing a specific receptor target; (ii) slow plasma kinetics with prolonged half-life and low breakdown of the supramolecular aggregates, both probably due to the presence of PEG moieties on the aggregate external surface, that appear useful for maintaining high blood concentrations of the desired agent.

Finally, new supramolecular aggregates have been developed [149] based on a new monomer with an upsilon shape (Fig. 9, compound **g**, MonY) that contains, in the same molecule, all the three fundamental tasks that are required: (a) the hydrophobic moiety that allows the formation of supramolecular aggregates, (b) the bioactive CCK8 peptide for target recognition, (c) a chelating agent able to give stable gadolinium complexes. MonY, and its gadolinium complex MonY(Gd), aggregate in water solution giving ellipsoidal micelles with the ratio between the micellar axis of ∼1.7 and the aggregation number N_{agg} of ∼30. There are no differences in the aggregation behaviour between MonY and MonY(Gd) indicating that the presence of metal ions and therefore the reduction of the net charge does not influence the aggregation behaviour. When MonY(Gd) are blended with DOPC, the aggregation behaviour is dictated by the tendency of DOPC in giving liposomes. Only when the amount of MonY(Gd), is higher than 20% the coexistence of liposomes and micelles is observed. The thickness d of the bilayer has been valuated by SANS to be ≈35–40 Å, whereas cryo-TEM images have shown that the diameter of the liposomes ranges between ≈50 and 150 nm. The relaxivity values per each gadolinium complex of self assembling micelles of MonY(Gd) and DOPC/MonY(Gd) liposomes (80:20 molar ratio) are 15.03 and 12.7 $mM^{-1}\,s^{-1}$, respectively. Gadolinium complexes in the inner and in the outer liposomal layers contribute at the same way to the paramagnetic relaxation rate. In fact, the presence of an unsaturation in the hydrocarbon chain of DOPC phospholipids increases the membrane permeability, thus facilitating the water flux across the bilayer [106].

6. Conclusions

The *in vivo* applicability of supramolecular aggregates, such as micelles and liposomes, containing Gd(III) complexes as contrast agents in MRI has been well documented. There are several reports that have approached and optimized issues of stability, relaxivity and overall safety for *in vivo* applications. The possibility of using micellar or liposomal compounds for imaging pourpose depends on the degree of stability of the imaging agent in the body. Liposomes show high stability in biological fluid, while micellar stability depends by its critical micellar concentration. Physiologically stable micelles (cmc value in a micromolar or low millimolar region) can be performed by using either monomers with two or more alkyl chains, or by polymerizable amphiphilic Gd(III) complexes. High contrast efficacy can be achieved by designing supramolecular paramagnetic MR-contrast agents characterized by high rigidity and good access of bulk water to the paramagnetic center. High rigidity can be obtained combining together a restricted motion of the contrast agent of the amphiphilic gadolinium complexes in the aggregate and a high molecular weight of the particle. These two effects will normally increase the contrast efficacy by prolonging

the rotational correlation time of the Gd(III) complex. Fast exchange between the water molecule coordinated to the gadolinium ion and the bulk water can be easily achieved if the Gd(III) complexes are exposed on the external surface of the aggregate, i.e., micelles; or in the case of liposomes by using a fluid membrane, which allows high water transport across the membrane. The water flux across the liposome bilayer depends by the length of the phospholipid alkyl chain and by the presence of unsaturations in the hydrocarbon chain and by the addition of cholesterol. Future work will also have to address how to optimize issues pertaining to the relationship of size and relaxivity. As it stands, the required size of the aggregates currently utilized that can produce relaxivity changes in a range suitable for current MRI scanners is fairly large. Issues concerning safety for *in vivo* use of such an approach need further investigation. Applications in which large amounts of high molecular weight contrast media can freely diffuse to selective targets, such as for example contrast-enhanced imaging of the vascular system or molecular targeting of integrins present on endothelial cells, have been very successful in animal models and may very well be successful in clinical use. On the other hand, permeability issues are likely to pose a major impairment for applications of molecular imaging in tissues where the target receptor or protein is not freely accessible. Reaching targets on tumour cells for example or in other tissues with permeability barriers will be very difficult and adequate concentrations of such aggregates for application in MRI are likely not to be achieved with currently available technology. However, given the rapid rate of progress in this field, it is likely that optimization of aggregate size and relaxivity will allow one to widen the range of molecular targeting applications with such an approach.

In conclusion, the development of novel MRI contrast agents based on supramolecular aggregates derivatized on the external surface by peptides or antibody should permit to couple high relaxivity and targeting selectivity on the same particle. Their envisioned use for the *in vivo*, non-invasive visualization of molecular markers should allow one to visualize diseases, for esample cancers, in the early stages of the transformation towards the malignant phenotype and to improve the quality of life. Moreover, administration of the targeted contrast agent should substantially reduce of deleterious side effects related to the imaging procedure.

Acknowledgments

Support from Network of Excellence *EMIL* (European Molecular Imaging Laboratories) is gratefully acknowledged. The authors are grateful to Prof. Luigi Paduano and co-workers for stimulating discussions on the structural parameters of the described aggregated systems, and Prof. Silvio Aime for giving us the opportunity to start our research in this field.

References

[1] I.R. Young, Methods in Biomedical Magnetic Resonance Imaging and Spectroscopy, John Wiley & Sons Ltd., Chichester, 2000.
[2] P.A. Rinck, Magnetic Resonance in Medicine, ABW Wissenschaftsverlag GmbH, Berlin, 2003.
[3] M.F. Tweedle, in: J.-C.G. Bünzli, G.R. Choppin (Eds.), Chemical and Earth Sciences: Theory and Practice, Elsevier, Amsterdam, 1989, p. 127.
[4] E. Brücher, A.D. Sherry, in: A.E. Merbach, E. Toth (Eds.), The Chemistry of Contrast Agents in Medical Magnetic Resonance Imaging, Wiley, Chichester, 2001, p. 243.
[5] H.J. Weinmann, A. Mühler, B. Radüchel, in: I.R. Young (Ed.), Biomedical Magnetic Resonance Imaging and Spectroscopy, John Wiley & Sons Ltd., Chichester, 2000, p. 705.
[6] R. Weissleder, M. Papisov, Rev. Magn. Reson. Med. 4 (1992) 1.
[7] L. Banci, I. Bertini, C. Luchinat, Nuclear and Electronic Relaxation, VCH, Weinheim, 1991.
[8] M. Botta, Eur. J. Inorg. Chem. 2000 (2000) 399.
[9] R.B. Lauffer, Chem. Rev. 87 (1987) 901.
[10] P. Caravan, J.J. Ellison, T.J. McMurry, R.B. Lauffer, Chem. Rev. 99 (1999) 2293.
[11] S. Aime, M. Botta, M. Fasano, E. Terreno, Chem. Soc. Rev. 27 (1998) 19.
[12] H. Schmitt-Willich, M. Brehm, C.L.J. Evers, G. Michl, A. Müller-Farnow, O. Petrov, J. Platzek, B. Radüchel, D. Sülzle, Inorg. Chem. 38 (1999) 1134.
[13] F. Uggeri, S. Aime, P.L. Anelli, M. Botta, M. Brocchetta, C. de Haën, G. Ermondi, M. Grandi, P. Paoli, Inorg. Chem. 34 (1995) 633.
[14] M. Bottrill, L. Kwok, N.J. Long, Chem. Soc. Rev. 35 (2006) 557.
[15] K.A. Deal, R. Motekaitis, A.E. Martell, M.J. Welch, J. Med. Chem. 39 (1996) 3096.
[16] S. Aime, M. Botta, M. Fasano, S. Geninatti Crich, E. Terreno, Coord. Chem. Rev. 321 (1999) 185.
[17] S. Aime, S. Geninatti Crich, E. Gianolio, G.B. Giovenzana, L. Tei, E. Terreno, Coord. Chem. Rev. 250 (2006) 1562.
[18] K. Wai-Yan Chan, Wing-Tak Wong, Coord. Chem. Rev. 251 (2007) 2428.
[19] M.P. Lowe, Aust. J. Chem. 55 (2002) 551.
[20] L. Frich, A. Bjornerud, S. Fossheim, T. Tillung, I. Gladhaug, Magn. Reson. Med. 52 (2004) 1302.
[21] M.P. Lowe, D. Parker, O. Reany, S. Aime, M. Botta, G. Castellano, E. Gianolio, R. Pagliarin, J. Am. Chem. Soc. 123 (2001) 7601.
[22] S.R. Zhang, K.C. Wu, A.D. Sherry, Angew. Chem. Int. Ed. 38 (1999) 3192.
[23] S. Aime, M. Botta, S. Geninatti Crich, G. Giovenzana, G. Palmisano, M. Sisti, Chem. Commun. (1999) 1577.
[24] S. Aime, M. Botta, E. Gianolio, E. Terreno, Angew. Chem. Int. Ed. 39 (4) (2000) 747.
[25] L. Burai, E. Toth, S. Seibig, R. Scopelliti, A.E. Merbach, Chem. Eur. J. 6 (20) (2000) 3761.
[26] E.L. Que, C.J. Chang, J. Am. Chem. Soc. 128 (2006) 15943.
[27] P.L. Anelli, I. Bertini, M. Fragai, L. Lattuada, C. Luchinat, G. Parigi, Eur. J. Inorg. Chem. 2000 (2000) 625.
[28] A.L. Nivorozhkin, A.F. Kolodziej, P. Caravan, M.T. Greenfield, R.B. Lauffer, T.J. McMurry, Angew. Chem. Int. Ed. 40 (2001) 2903.
[29] W.J.M. Mulder, G.J. Strijkers, A.W. Griffioen, L. van Bloois, G. Molema, G. Storm, G. Koning, K. Nicolay, Bioconjugate Chem. 15 (2004) 799.
[30] S.R. Bull, M.O. Guler, R.E. Bras, T.J. Maede, S.I. Stupp, Nano Lett. 5 (2005) 1.
[31] E. Battistini, E. Gianolio, R. Gref, P. Couvreur, S. Fuzerova, M. Othman, S. Aime, B. Badet, P. Durand, Chem. Eur. J. 14 (2008) 4551.
[32] S. Aime, M. Botta, E. Garino, S. Geninatti Crich, G. Giovenzana, R. Pagliarin, G. Palmisano, M. Sisti, Chem. Eur. J. 6 (2000) 2609.
[33] J. Li, D. Zheng, K.T. Bae, P.K. Woodard, E.M. Haacke, Invest. Radiol. 33 (1998) 578.
[34] A. Mühler, Invest. Radiol. 33 (1998) 709.
[35] A. Mühler, MAGMA 3 (1995) 21.
[36] P. Caravan, N.J. Cloutier, M.T. Greenfield, S.A. McDermid, S.U. Dunham, J.W.M. Bulte, J.C. Amedio Jr., R.J. Looby, R.M. Supkowski, W.D. Horrocks, T.J. McMurry, R.B. Lauffer, J. Am. Chem. Soc. 124 (2002) 3152.
[37] R.B. Lauffer, D.J. Parmelee, H.S. Ouellet, R.P. Dolan, H. Sajiki, D.M. Scott, P.J. Bernard, E.M. Buchanan, K.Y. Ong, Z. Tyeklar, K.S. Midelfort, T.J. McMurry, R.C. Walovitch, Acad. Radiol. 3 (1996) S356.
[38] T.M. Grist, F.R. Korosec, D.C. Peters, S. Witte, R.C. Walovitch, R.P. Dolan, W.E. Bridson, E.K. Yucel, C.A. Mistretta, Radiology 207 (1998) 539.
[39] A.W. Bosman, H.M. Janssen, E.W. Meijer, Chem. Rev. 99 (1999) 1665.
[40] D.L. Ladd, R. Hollister, X. Peng, D. Wei, G. Wu, D. Delecki, R.A. Snow, J.L. Toner, K. Kellar, J. Eck, V.C. Desai, G. Raymond, L.B. Kinter, T.S. Desser, D.L. Rubin, Bioconjugate Chem. 10 (1999) 361.
[41] S. Laus, B. Sitharaman, E. Toth, R.D. Bolskar, L. Helm, L.J. Wilson, A.E. Merbach, J. Phys. Chem. C 111 (2007) 5633.
[42] K.B. Hartman, S. Laus, R.D. Bolskar, R. Muthupillai, L.M. Helm, E. Toth, A.E. Merbach, L.J. Wilson, Nano Lett. 8 (2008) 415.
[43] S. Geninatti Crich, A. Barge, E. Battistini, C. Cabella, S. Coluccia, D. Longo, V. Mainero, G. Tarone, S. Aime, J. Biol. Inorg. Chem. 10 (2005) 78.
[44] H. Kobayaski, S. Kawamoto, S.-K. Jo, H.L. Bryant Jr., M.W. Brechbiel Jr., R.A. Star, Bioconjugate Chem. 14 (2003) 388.
[45] S. Langereis, Q.G. de Lussanet, M.H.P. van Genderen, W.H. Baches, E.W. Meijer, Macromolecules 37 (2004) 3084.
[46] S. Langereis, A. Dirksen, T.M. Hackeng, M.H.P. van Genderen, E.W. Meijer, New J. Chem. 31 (2007) 1152.
[47] Q. Dong, D.R. Hurst, H.J. Weinmann, T.L. Chenevert, F.J. Londy, M.R. Prince, Invest. Radiol. 33 (1998) 699.
[48] T.S. Desser, D.L. Rubin, H. Muller, G.L. McIntire, E.R. Bacon, K.R. Hollister, Acad. Radiol. 6 (1999) 112.
[49] H. Kato, Y. Kanazawa, M. Okumura, A. Taninaka, T. Yokawa, H. Shinohara, J. Am. Chem. Soc. 125 (2003) 4391.
[50] P.P. Fatouros, F.D. Frank, Z. Chen, W.C. Brosddus, J.L. Tatum, B. Kettenmann, Z. Ge, H.W. Gibson, J.L. Russ, A.P. Leonard, J.C. Duchamp, H.C. Dorn, Radiology 204 (2006) 756.
[51] E. Toth, R.D. Bolskar, A. Borel, G. Gonzales, L.M. Helm, A.E. Merbach, B. Sitharaman, L.J. Wilson, J. Am. Chem. Soc. 127 (2005) 799.
[52] R.D. Bolskar, A.F. Benedetto, L.O. Husebo, R.E. Price, E.F. Jackson, S. Wallace, L.J. Wilson, J.N. Alford, J. Am. Chem. Soc. 125 (2003) 5471.
[53] C. Richard, B.T. Doan, J.C. Beloeil, M. Bessodes, E. Toth, D. Scherman, Nano Lett. 8 (2008) 232.
[54] A. Dirksen, S. Langereis, B.F.M. de Waal, M.H.P. van Genderen, T.M. Hackeng, E.W. Meijer, Chem. Commun. (2005) 2811.
[55] D. Artemov, N. Mori, R. Ravi, Z.M. Bhujwalla, Cancer Res. 63 (2003) 2723.
[56] S. Aime, E. Gianolio, E. Terreno, I. Menegotto, C. Bracco, L. Milone, G. Cravotto, Magn. Reson. Chem. 41 (2003) 800.
[57] V. Degiorgio, Physics of Amphiphiles: Micelles, Vesicles and Microemulsions, Amsterdam, 1985.

[58] J.N. Israelachvilli, D.J. Mitchell, B.W. Ninham, J. Chem. Soc., Faraday Trans. 2: Mol. Chem. Phys. 72 (1976) 1525.
[59] M. Jones, J. Leroux, Eur. J. Pharm. Biopharm. 48 (1999) 101.
[60] A. Martin (Ed.), Physical Pharmacy, Lippinkott, Williams and Wilkins, Philadelphia, 1993.
[61] V.P. Torchilin, Nat. Rev. Drug Discov. 4 (2005) 145.
[62] D.C. Drummond, O. Meyer, K. Hong, D.B. Kirpotin, D. Papahadjopoulos, Pharmacol. Rev. 51 (1999) 691.
[63] D.D. Lasic, Nature 355 (1992) 279.
[64] R.J. Hunter (Ed.), Introduction to Modern Colloid Science, Oxford University Press, Oxford, UK, 1993.
[65] A. Martinez-Coscolla, E. Miralles-Loyola, T.M. Garrigues, M.D. Sirvent, E. Salinas, V.G. Casabo, Drug. Res. 43 (1993) 699.
[66] G.S. Kwon, K. Kataoka, Adv. Drug Deliv. Rev. 16 (1995) 295.
[67] C. Tilcock, E. Unger, P. Cullis, P. MacDougall, Radiology 171 (1989) 77.
[68] G. Kabalka, E. Buonocore, K. Hubner, T. Moss, N. Norley, L. Huang, Radiology 163 (1987) 255.
[69] C.W.M. Grant, S. Karlik, E.A. Florio, Magn. Reson. Med. 11 (1989) 236.
[70] E. Unger, T. Fritz, G. Wu, D. Shen, B. Kulik, T. New, M. Crowell, N. Wilke, J. Liposome Res. 4 (1994) 811.
[71] E. Unger, D.K. Shen, G.L. Wu, T. Fritz, Magn. Reson. Med. 22 (1991) 304.
[72] S.H. Koenig, Q.F. Ahkong, R.D. Brown III, M. Lafleur, M. Spiller, E. Unger, C. Tilcock, Magn. Reson. Med. 23 (1992) 275.
[73] G.W. Kabalka, M.A. Davis, E. Buonocore, K. Hubner, E. Holmberg, L. Huang, Invest. Radiol. 25 (1990) S63.
[74] G.W. Kabalka, M.A. Buonocore, K. Hubner Davis, E.L. Huang, Magn. Reson. Med. 8 (1988) 89.
[75] C.W.M. Grant, S. Karlik, E. Florio, Magn. Reson. Med. 11 (1989) 236.
[76] G. Kabalka, E. Buonocore, K. Hubner, M. Davis, L. Huang, Magn. Res. Med. 8 (1989) 89.
[77] S.K. Kim, G.M. Pohost, G.A. Elgavish, Magn. Reson. Med. 22 (1991) 57.
[78] G. Lipari, A. Szabo, J. Am. Chem. Soc. 104 (1982) 4546.
[79] G. Lipari, A. Szabo, J. Am. Chem. Soc. 104 (1982) 4559.
[80] J.P. Andre, E. Toth, H. Fischer, A. Seelig, H.R. Macke, A.E. Merbach, Chem. Eur. J. 5 (1999) 2977.
[81] G.M. Nicolle, E. Toth, K.P. Eisenwiener, H.R. Macke, A.E. Merbach, J. Biol. Inorg. Chem. 7 (2002) 757.
[82] R. Hovland, C. Gløgård, A.J. Aasen, J. Klaveness, Org. Biomol. Chem. 1 (2003) 644.
[83] G.M. Nicolle, L. Helm, A.E. Merbach, Magn. Reson. Chem. 41 (2003) 794.
[84] E. Gianolio, G.B. Giovenzana, D. Longo, I. Longo, I. Menegotto, S. Aime, Chem. Eur. J. 13 (2007) 5785.
[85] M.I. Torres, M. Prata, A.C. Santos, J.P. André, J.A. Martins, L. Helm, É. Tóth, M.L. García-Martín, T.B. Rodrigues, P. López-Larrubia, S. Cerdán, C.F.G.C. Geraldes, NMR Biomed. 21 (2008) 322.
[86] S. Torres, J.A. Martins, J.P. Andre, C.F.G.C. Geraldes, A.E. Merbach, E. Toth, Chem. Eur. J. 12 (2006) 940.
[87] G. Schuhmann Giampieri, H. Schmitt-Willich, W.R. Press, C. Negishi, H.J. Weinmann, U. Speck, Radiology 183 (1992) 59.
[88] G. Vittadini, E. Felder, C. Musu, C. Tirone, Invest. Radiol. 5 (1990) S59.
[89] M. Vaccaro, A. Accardo, D. Tesauro, G. Mangiapia, D. Löf, K. Schillén, O. Söderman, G. Morelli, L. Paduano, Langmuir 22 (2006) 6635.
[90] A. Accardo, D. Tesauro, G. Morelli, E. Gianolio, S. Aime, M. Vaccaro, G. Mangiapia, L. Paduano, K. Schillen, J. Biol. Inorg. Chem. 12 (2007) 267.
[91] R.W. Storrs, F.D. Tropper, H.Y. Li, C.K. Song, J.K. Kuniyoshi, D.A. Sipkins, K.C.P. Li, M.D. Bednarski, J. Am. Chem. Soc. 117 (1995) 7301.
[92] L. Lattuada, G. Lux, Tetrahedron Lett. 44 (2003) 3893.
[93] O. Morag, A. Ahmad, N. Kamaly, E. Perouzel, A. Caussin, M. Keller, A. Herlihy, J. Bell, A.D. Miller, M.R. Jorgensen, Org. Biomol. Chem. 4 (2006) 3489.
[94] K.S. Kim, G.M. Pohost, G.A. Elgavish, Bioconjugate Chem. 3 (1992) 20.
[95] W.J. Chu, T. Simor, G.A. Elgavish, NMR Biomed. 10 (1997) 87.
[96] T. Simor, W.J. Chu, L. Johnson, A. Safranko, M.P. Doyle, G.M. Pohost, G.A. Elgavish, Circulation 92 (1995) 3549.
[97] C. Gløgård, R. Hovland, S.L. Fossheim, A.J. Aasen, J. Klaveness, J. Chem. Soc. Perkin Trans. 2 (2000) 1047.
[98] C. Gløgård, G. Stensrud, R. Hovland, S.L. Fossheim, J. Klaveness, Int. J. Pharm. 233 (2002) 131.
[99] C. Gløgård, G. Stensrud, J. Klaveness, Int. J. Pharm. 253 (2003) 39.
[100] K. Kimpe, T.N. Parac-Vogt, S. Laurent, C. Pierart, L.V. Elst, R.N. Muller, K. Binnemans, Eur. J. Inorg. Chem. (2003) 3021.
[101] T.N. Parac-Vogt, K. Kimpe, S. Laurent, C. Pierart, L.V. Elst, R.N. Muller, Eur. J. Inorg. Chem. 2004 (2004) 3538.
[102] T.N. Parac-Vogt, K. Kimpe, S. Laurent, C. Pierart, V.L. Elst, R.N. Muller, K. Binnemans, Eur. Biophys. J. 35 (2006) 136.
[103] F. Botteman, G.N. Nicolle, L.V. Elst, S. Laurent, A.E. Merbach, R.N. Muller, Eur. J. Inorg. Chem. 2000 (2002) 2686.
[104] S. Laurent, V.L. Elst, C. Thirifays, R.N. Muller, Eur. Biophys. J. 37 (2008) 1007.
[105] D. Huster, A.J. Jin, K. Arnold, K. Gawrisch, Biophys. J. 73 (1997) 855.
[106] F. Alhaique, I. Bertini, M. Fragai, M. Carafa, C. Luchinat, G. Parigi, Inorg. Chim. Acta 331 (2002) 151.
[107] S. Laurent, L.V. Elst, C. Thirifays, R.N. Muller, Langmuir 24 (2008) 4347.
[108] P.L. Anelli, L. Lattuada, V. Lorusso, M. Schneider, H. Tournier, F. Uggeri, MAGMA 12 (2001) 114.
[109] H. Tournier, R. Hyacinthe, M. Schneider, Acad. Radiol. 9 (2002) S20.
[110] E. Terreno, A. Sanino, C. Carrera, D. Delli Castelli, G.B. Giovenzana, A. Lombardi, R. Mazzon, L. Milone, M. Visigalli, S. Aime, J. Inorg. Biochem. 102 (2008) 1112.
[111] C. Tilcock, Adv. Drug Deliv. Rev. 37 (1999) 33.
[112] G.J. Strijkers, W.J.M. Mulder, R.B. van Heeswijk, P.M. Frederik, P. Bomans, P.C.M.M. Magusin, K. Nicolay, Magn. Reson. Mater. Phys. 18 (2005) 186.
[113] C. Gløgård, G. Stensrud, S. Aime, Magn. Reson. Chem. 41 (2003) 585.
[114] N. Kamaly, T. Kalber, A. Ahmad, M.H. Oliver, P.W. So, A.H. Herlihy, J.D. Bell, M.R. Jorgensen, A.D. Miller, Bioconjugate Chem. 19 (2008) 118.
[115] V. Weissig, J. Babich, V.P. Torchilin, Colloids Surf. B: Biointerf. 18 (2000) 293.
[116] V.S. Trubetskoy, J.A. Cannillo, A. Milshtein, G.L. Wolf, V.P. Torchilin, Magn. Reson. Imag. 13 (1995) 31.
[117] A.L. Klibanov, K. Maruyama, V.P. Torchilin, L. Huang, FEBS Lett. 268 (1990) 235.
[118] H.M. Patel, S.M. Moghimi, in: G. Gregoriadis, A.C. Allison, G. Poste (Eds.), Targeting of Drugs – Optimization Strategies, Plenum Press, New York, 1990, p. 87.
[119] W.J.M. Mulder, G.J. Strijkers, J.W. Habets, E.J.W. Bleeker, D.W.J. van der Schaft, G. Storm, G.A. Koning, A.W. Griffioen, K. Nicolay, FASEB J. 19 (2005) 2008.
[120] V.P. Torchilin, J. Controll. Release 73 (2001) 137.
[121] G.S. Kwon, Crit. Rev. Ther. Drug Carr. Syst. 20 (2003) 357.
[122] J.M. Harris, N.E. Martin, M. Modi, Clin. Pharmacokinet. 40 (2001) 539.
[123] D.W. Miller, E.V. Batrakova, T.O. Waltner, V.Yu. Alakhov, A.V. Kabanov, Bioconjugate Chem. 8 (1997) 649.
[124] S. Katayose, K. Kataoka, J. Pharm. Sci. 87 (1998) 160.
[125] A. Harada, K. Kataoka, Macromolecules 31 (1998) 288.
[126] G.S. Kwon, M. Naito, M. Yokoyama, T. Okano, Y. Sakurai, K. Kataoka, J. Control. Release 48 (1997) 195.
[127] Y.I. Jeong, J.B. Cheon, S.H. Kim, J.W. Nah, Y.M. Lee, Y.K. Sung, J. Control. Release 51 (1998) 169.
[128] A.V. Kabanov, V.A. Kabanov, Adv. Drug Deliv. Rev. 30 (1998) 49.
[129] V.P. Torchilin, Curr. Pharm. Biotechnol. 1 (2000) 183.
[130] E. Nakamura, K. Makino, T. Okano, T. Yamamoto, M. Yokoyama, J. Control. Release 114 (2006) 325.
[131] H.Y. Lee, H.W. Jee, S.M. Seo, B.K. Kwak, G. Khang, S.H. Cho, Bioconjugate Chem. 17 (2006) 700.
[132] J.L. Turner, D. Pan, R. Plummer, Z. Chen, A.K. Whittaker, K.L. Wooley, Adv. Funct. Mater. 15 (2005) 1248.
[133] W.J.M. Mulder, G.J. Strijkers, K.C. Briley-Saebo, J.C. Frias, J.G.S. Aguinado, E. Vudic, V. Amirbekian, C. Tang, P.T.K. Chin, K. Nicolay, Z.A. Fayad, Magn. Reson. Med. 58 (2007) 1164.
[134] M.J. Lipinski, V. Amirbekian, J.C. Frias, J.G.S. Aguinado, V. Mani, K.C. Briley-Saebo, V. Fuster, J.T. Fallon, E.A. Fisher, Z.A. Fayad, Magn. Reson. Med. 56 (2006) 601.
[135] V. Amirbekian, M.J. Lipinski, K.C. Briley-Saebo, S. Amirbekian, J.G.S. Aguinado, D.B. Weinreb, E. Vucic, J.C. Frias, F. Hyafil, V. Mani, E.A. Fisher, Z.A. Fayad, Proc. Natl. Acad. Sci. 104 (2007) 961.
[136] K.C.P. Li, M.D. Bednarski, J Magn. Res. Imag. 16 (2002) 388.
[137] D.A. Sipkins, D.A. Cheresh, M.R. Kazemi, L.M. Nevin, M.D. Bednarski, K.C.P. Li, Nat. Med. 4 (1998) 623.
[138] D.A. Sipkins, K. Gijbels, F.D. Tropper, M.D. Bednarski, K.C.P. Li, L. Steinman, J. Neuroimmunol. 104 (2000) 1.
[139] S.R. Bull, M.O. Guler, R.E. Bras, P.N. Venkatasubramanian, S.I. Stupp, T.J. Maede, Bioconjugate Chem. 16 (2005) 1343.
[140] G.A.F. van Tilborg, W.J.M. Mulder, N. Deckers, G. Storm, C.P.M. Reutelingsperger, G.J. Strijkers, K. Nicolay, Bioconjugate Chem. 17 (2006) 741.
[141] A.H. Schmieder, P.M. Winter, S.D. Caruthers, T.D. Harris, T.A. Williams, J.S. Allen, E.K. Lacy, H. Zhang, M.J. Scott, G. Hu, J.D. RObertson, S.A. Wickline, G.M. Lanza, Magn. Reson. Med. 53 (2005) 621.
[142] W.J.M. Mulder, D.W.J. van der Schaft, P.A.I. Hautvast, G.J. Strijkers, G.A. Koning, G. Storm, K.H. Mayo, A.W. Griffioen, K. Nicolay, FASEB J. 21 (2007) 378.
[143] R.J.M.G.E. Brandwijk, W.J.M. Mulder, K. Nicolay, K.H. Mayo, V.L.J.L. Thijssen, A.W. Griffioen, Bioconjugate Chem. 18 (2007) 785.
[144] W.J.M. Mulder, R.J.M.G.E. Brandwijk, G. Storm, P.T.K. Chin, G.J. Strijkers, C.D.M. Donerà, K. Nicolay, A.W. Griffioen, Nano Lett. 6 (2006) 1.
[145] T. Ke, E.K. Jeong, X Wang, Y. Feng, D. Parker, Z.R. Lu, Int. J. Nanomed. 2 (2007) 191.
[146] A. Accardo, D. Tesauro, P. Roscigno, E. Gianolio, L. Paduano, G. D'Errico, C. Pedone, G. Morelli, J. Am. Chem. Soc. 126 (2004) 3097.
[147] G. Mangiapia, A. Accardo, F. Lo Celso, D. Tesauro, G. Morelli, A. Radulescu, L. Paduano, J. Phys. Chem. B 108 (2004) 17611.
[148] D. Tesauro, A. Accardo, E. Gianolio, L. Paduano, J. Teixeira, K. Schillen, S. Aime, G. Morelli, ChemBioChem 8 (2007) 950.
[149] M. Vaccaro, G. Mangiapia, L. Paduano, E. Gianolio, A. Accardo, D. Tesauro, ChemPhysChem 8 (2007) 2526.
[150] D. Mierke, C. Giragossian, Med. Res. Rev. 21 (2001) 450.
[151] J.C. Reubi, B. Waser, Cancer Res. 57 (1997) 1377.
[152] A. Accardo, D. Tesauro, L. Aloj, L. Tarallo, C. Arra, G. Mangiapia, M. Vaccaro, C. Pedone, L. Paduano, G. Morelli, Chem. Med. Chem. 3 (2008) 594.